this finding was consistent with previous reports (ref. 11; Fig. 1*A*). The levels of *survivin* mRNA, however, varied widely among the different cancer cell lines. *Survivin* mRNA expression was remarkably high in both hepatoma cell lines tested, HepG2 and Hep3B, and in one of the osteosarcoma cell lines, SaOS-2. The levels in the other cell lines were only moderate or relatively low. *Survivin* mRNA was also detected in normal WI-38 human fibroblasts and primary human osteoblasts; these levels, however, were relatively low in comparison to those seen in the cancer cell lines.

Strong cancer-specific activity of the *survivin* promoter. The *survivin* promoter provided strong transcriptional activation in all of the cancer cell lines that showed sufficient viral transduction (Fig. 1*B*). The low levels or absence of β-gal activity after infection with adenoviruses in either Colo-205 or KHOS-NP cells was apparently due to very low levels of AGTE in these cells and not to a low activity of the *survivin* promoter. β-gal activity was not detected in this group even after infection with Ad.RSV-LacZ or Ad.CMV-LacZ at the same MOI (MOI of 30). The apparent variability in β-gal levels was also due to both the variability of AGTE levels in individual cells and the cellular activity required to express the transgenes and not the variability in *survivin* promoter activity. In seven of the remaining nine cancer cell lines, the *survivin* promoter exhibited stronger activity than either the RSV promoter or the CMV promoter, two representative ubiquitously strong promoters (27, 28). Notably, the *survivin* promoter was stronger than both the RSV and CMV promoters in HepG2 cells. In two additional cell lines, HCT-15 and LoVo, the *survivin* promoter displayed activity levels very similar to those observed for the RSV and CMV promoters.

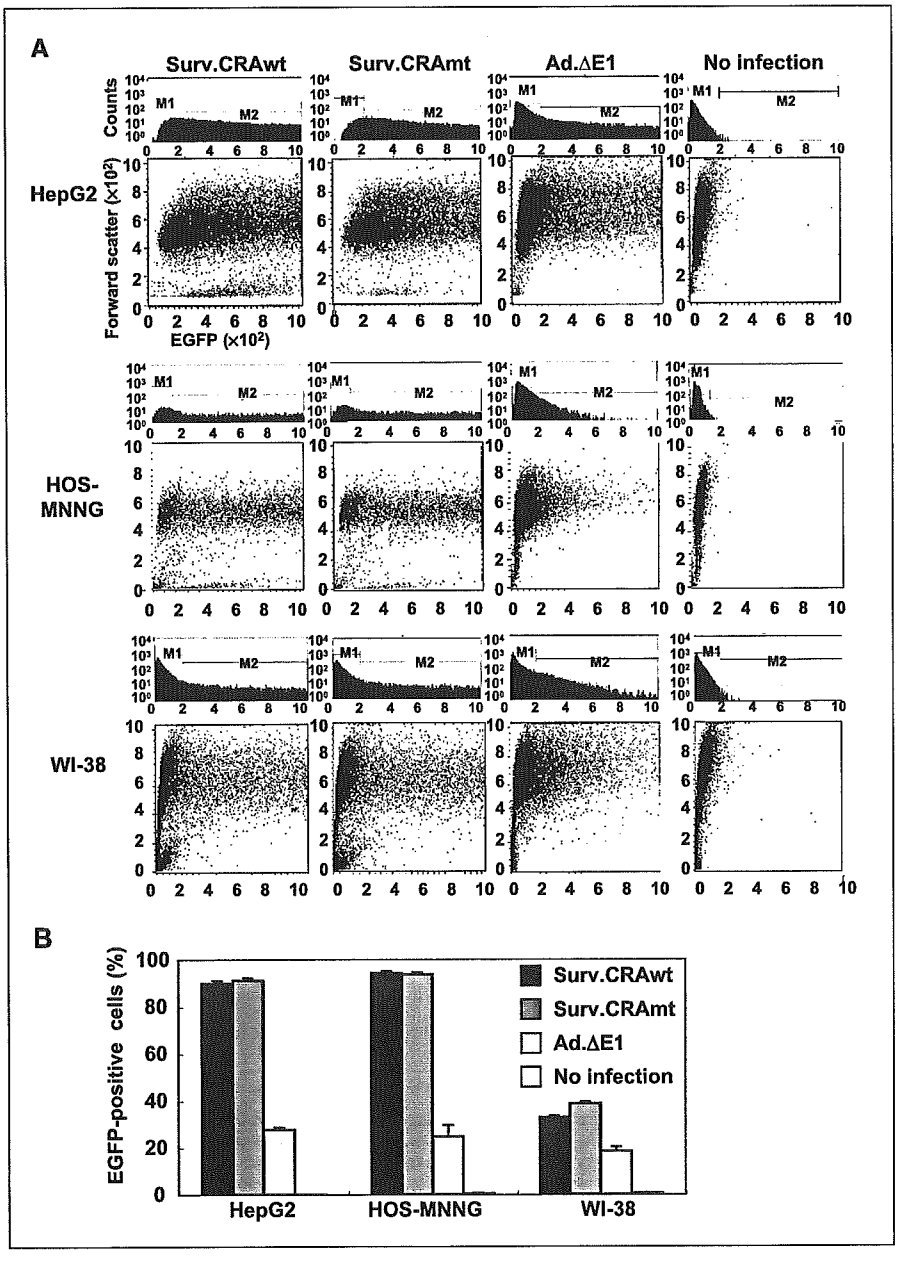

Figure 3. Flow cytometric analysis of EGFP-positive cells. HepG2, HOS-MNNG, and WI-38 cells were infected with Surv.CRAwt, Surv.CRAmt, or Ad.ΔE1 at an MOI of 0.1 (HepG2) or 1 (HOS-MNNG and WI-38). Twenty-four hours later, cells were fixed with 4% paraformaldehyde; the percentage of EGFP-positive cells was analyzed by flow cytometry. *A*, histograms (*top*) of EGFP-positive cells (M1, negative; M2, positive) and dot plots (*bottom*) individually representing the EGFP intensity and the forward scatter index. *B*, *columns*, percentages of EGFP-positive cells (mean of three independent experiments); *bars*, ±SE.

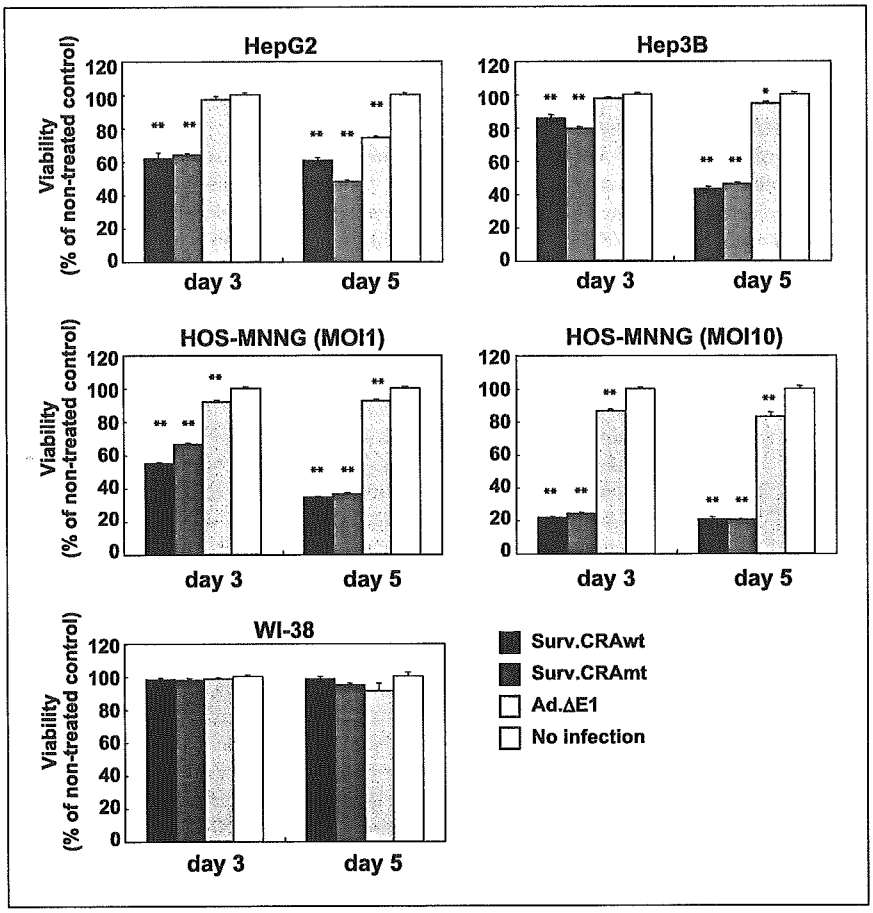

Figure 4. Cytotoxic effects *in vitro*. Cells were infected with Surv.CRAwt, Surv.CRAmt, or Ad.ΔE1 at an MOI of 0.1 in HepG2 and Hep3B cells, MOIs of 1 and 10 in HOS-MNNG cells, and an MOI of 1 in WI-38 cells. Cell viability was determined by WST-8 assay 3 or 5 days after infection. *, $P < 0.05$ and **, $P < 0.001$ (statistical significance in comparison with the no-infection control).

In contrast, *survivin* promoter activity was not detected in normal WI-38 fibroblasts despite both high levels of RSV and CMV promoter activity and moderate to high AGTE levels. Despite detectable, albeit low, levels of endogenous *survivin* expression, no detectable transactivation could be observed in normal cells with the use of this *survivin* promoter (Fig. 1*B*). Thus, the *survivin* promoter region and length of the transcriptional regulatory element used in these experiments are suitable to induce strong transactivation in all cancer types examined here in a tumor-specific manner.

Surv.CRAs efficiently and selectively replicated in cancer. After infection with Surv.CRAwt or Surv.CRAmt, the number of EGFP-positive cells increased in a time-dependent manner in all of the cancer cell lines analyzed, indicating the efficient replication of both Surv.CRAs (Fig. 2). Cytopathic effect was efficiently induced within a short period of time after the appearance of EGFP positivity. The speed of the Surv.CRA spreading was consistent with the observed levels of β-gal activity (Fig. 1*B*), except for MKN-45 cells. In these cells, the Surv.CRAs replicated very rapidly, spreading throughout the entire culture dish at a rate similar to that seen in LoVo, HepG2, and Hep3B cells. The slow yet still apparent spread of the Surv.CRAs was even observed in Colo-205 cells, despite a low AGTE in the initial infection. This phenomenon likely results from high levels of endogenous *survivin* expressed, suggesting that efficient viral replication within cells may overcome the disadvantage of low AGTE. In contrast, the percentage of EGFP-positive cells did not clearly increase over a 7-day period in normal WI-38 cells, although the EGFP fluorescence intensity within each cell increased minimally. In addition, no cytopathic effect was observed in WI-38 cells even at 7 days after infection with Surv.CRAs.

To verify tumor-specific replication of both Surv.CRAs accurately and quantitatively, we did flow cytometric analysis using two representative cancer cell lines, HepG2 and HOS-MNNG, as well as normal WI-38 cells. HepG2 cells exhibited the highest levels of *survivin* expression, the highest AGTE levels, and the strongest *survivin* promoter activity, resulting in rapid amplification of the Surv.CRAs (Fig. 2). HOS-MNNG showed low to moderate levels of these properties, resulting in lower but significant viral replication. Twenty-four hours after infection with either of the adenoviruses at the MOI that initially provided approximately 20% AGTE, Surv.CRAs propagated rapidly, spreading to >90% of HepG2 and HOS-MNNG cells. Under these conditions, we could not observe any significant amplification or spread of the control replication-defective Ad.ΔE1 (Fig. 3). In contrast, the propagation and resulting spread of Surv.CRAs remained minimal in WI-38 cultures. Thus, both Surv.CRAs replicated more efficiently in cancer cells, even those expressing *survivin* at relatively low levels, with moderate AGTE levels, than in normal WI-38 cells. In addition, we did not detect any significant differences in the phenotypic characteristics of Surv. CRAwt and Surv.CRAmt in any of the cell types tested.

Surv.CRAs specifically kill cancer cells *in vitro*. To assess the selective killing of cancer cells by Surv.CRAs, we conducted a cell viability assay (Fig. 4). In two representative cell lines showing both high AGTE and high levels of *survivin* expression, HepG2 and Hep3B cells, Surv.CRAs induced prominent cytotoxic effects as

early as 3 days, even when infection was done at a low MOI (0.1). Both hepatoma cell lines were sensitive to adenoviral cytotoxicity; cytotoxic effects were minimally but clearly seen 5 days after infection at an MOI of 0.1 with the control, E1-deleted Ad.ΔE1. In HOS-MNNG cells, which exhibited low expression of *survivin* and moderate AGTE levels, both Surv.CRAs induced more prominent cytotoxicity than Ad.ΔE1. The cytotoxic effects were amplified in a dose-dependent manner when initial infection at increasingly higher MOI (Fig. 4). In contrast to these results in cancer cell lines, neither Surv.CRA induced cytotoxic effects in normal WI-38 fibroblast cells, even 5 days after infection at an MOI of 1. Thus, both Surv.CRAs efficiently induced cell death in three cancer cell lines in contrast to the lack of clear toxicity observed in normal WI-38 cells. In addition, we did not observe any significant differences in the cytotoxicity of Surv.CRAwt and Surv.CRAmt between the cell types tested, including the normal WI-38 cells, RB-intact HepG2 cells, and RB-deficient Hep3B cells.

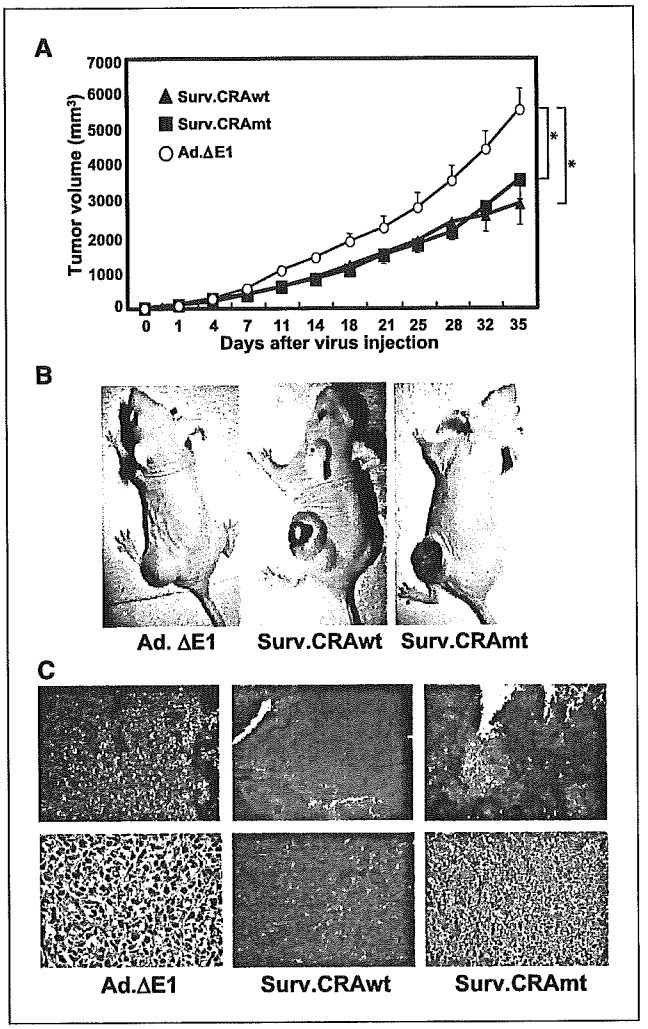

Figure 5. Therapeutic effects of Surv.CRAs *in vivo*. *A*, tumor volume was measured after a single injection of 1×10^8 pfu Surv.CRAwt ($n = 9$), Surv.CRAmt ($n = 8$), or control Ad.ΔE1 ($n = 8$) into preestablished s.c. tumors of HOS-MNNG cells in nude mice. *, $P < 0.05$ (statistical significance in comparison with infection with the control Ad.ΔE1). *B*, representative macroscopic pictures 14 days after injection of Ad.ΔE1, Surv.CRAwt, or Surv.CRAmt. Prominent tumor necrosis was apparent in Surv.CRAwt- and Surv.CRAmt-treated masses. *C*, representative histologic images at the time of sacrifice. H&E-stained sections exhibited large necrotic areas in the tumor nodules in mice treated with either Surv.CRA. In contrast, tumor nodules contained primarily viable tumor cells without large necrotic areas in the Ad.ΔE1-treated mice. Original magnification: ×20 (*top*) and ×100 (*bottom*). Both the macroscopic and microscopic pictures provide a more accurate assessment of the therapeutic potential of the Surv.CRAs than the simple assessment of tumor volume.

Surv.CRA inhibited tumor growth *in vivo*. Using an animal model of preestablished s.c. tumors, we examined the therapeutic potential of both Surv.CRAs *in vivo*. We intentionally used an HOS-MNNG osteosarcoma cell line that expressed relatively low levels of *survivin* and showed moderate levels of AGTE to assess the therapeutic potentials of these vectors in a wider range of cancers. A single intratumoral administration (1×10^8 pfu) of Surv.CRAwt or Surv.CRAmt significantly inhibited tumor growth in comparison to the same dose of Ad.ΔE1 (Fig. 5*A*). Statistically significant differences in the tumor size were seen between Surv.CRAs-treated and Ad.ΔE1-treated mice as early as 11 days after administration and continuing thereafter. As assessed by macroscopic and microscopic examination, the therapeutic effects of both Surv.CRAs were more significant; the tumor nodules in Surv.CRA-treated mice contained large necrotic areas, whereas the nodules in Ad.ΔE1-treated mice consisted primarily of viable tumor cells histologically showing active malignant features (Fig. 5*B* and *C*). These results suggest the therapeutic potential and general utility of Surv.CRAs for the treatment of cancer.

The superiority of Surv.CRAs to a Tert.CRA. We compared the viral properties of Surv.CRAs with those of Tert.CRA. The expression levels of endogenous TERT varied among cancer cell lines; HOS-MNNG cells, as well as HepG2 cells, expressed TERT mRNA at very high levels (Fig. 6*A*), in contrast to the relatively low level of *survivin* expression in HOS-MNNG cells (Fig. 1*A*). Nevertheless, the activity of the *survivin* promoter in HOS-MNNG cells was higher than that of the TERT promoter, as well as in HepG2 cells (Fig. 6*B*). These results suggest that the *survivin* promoter may be more active than the TERT promoter among multiple cancer cell types.

To precisely analyze the differences in the efficiency and attenuation of viral replication between Surv.CRAs and Tert.CRA in cancerous and normal cells, we did flow cytometric analysis after infection of three types of cells at low MOI (Fig. 6*C*). Surv.CRAwt exhibits more efficient replication in both HepG2 and HOS-MNNG cells than that seen in Tert.CRAwt cells, although the former virus is more quiescent in normal WI-38 cells than the latter.

We compared the therapeutic potentials of Surv.CRAwt and Tert.CRAwt in tumor-bearing animals (Fig. 6*D*). Although we did not find a statistically significant difference in the effects of Surv.CRAwt and Tert.CRAwt, both viruses significantly decreased tumor size in animals from the tumor volumes observed in mice treated with the control Ad.ΔE1 virus. Tumor volumes in Surv.CRAwt-treated mice were smaller than those in Tert.CRAwt-treated animals; in addition, the difference between the Surv.CRAwt and control Ad.ΔE1 groups was more significant (smaller P) than the difference between the Tert.CRAwt and Ad.ΔE1 groups.

Discussion

This study provides the first report of two *survivin*-responsive CRAs, both showing efficient cancer-specific replication and potent therapeutic effects against cancers both *in vitro* and *in vivo*.

One of the attractive features of Surv.CRAs is their ability to target a variety of cancers. Surv.CRAs showed efficient propagation and induced cell death in a wide variety of tumor cells with a variety of

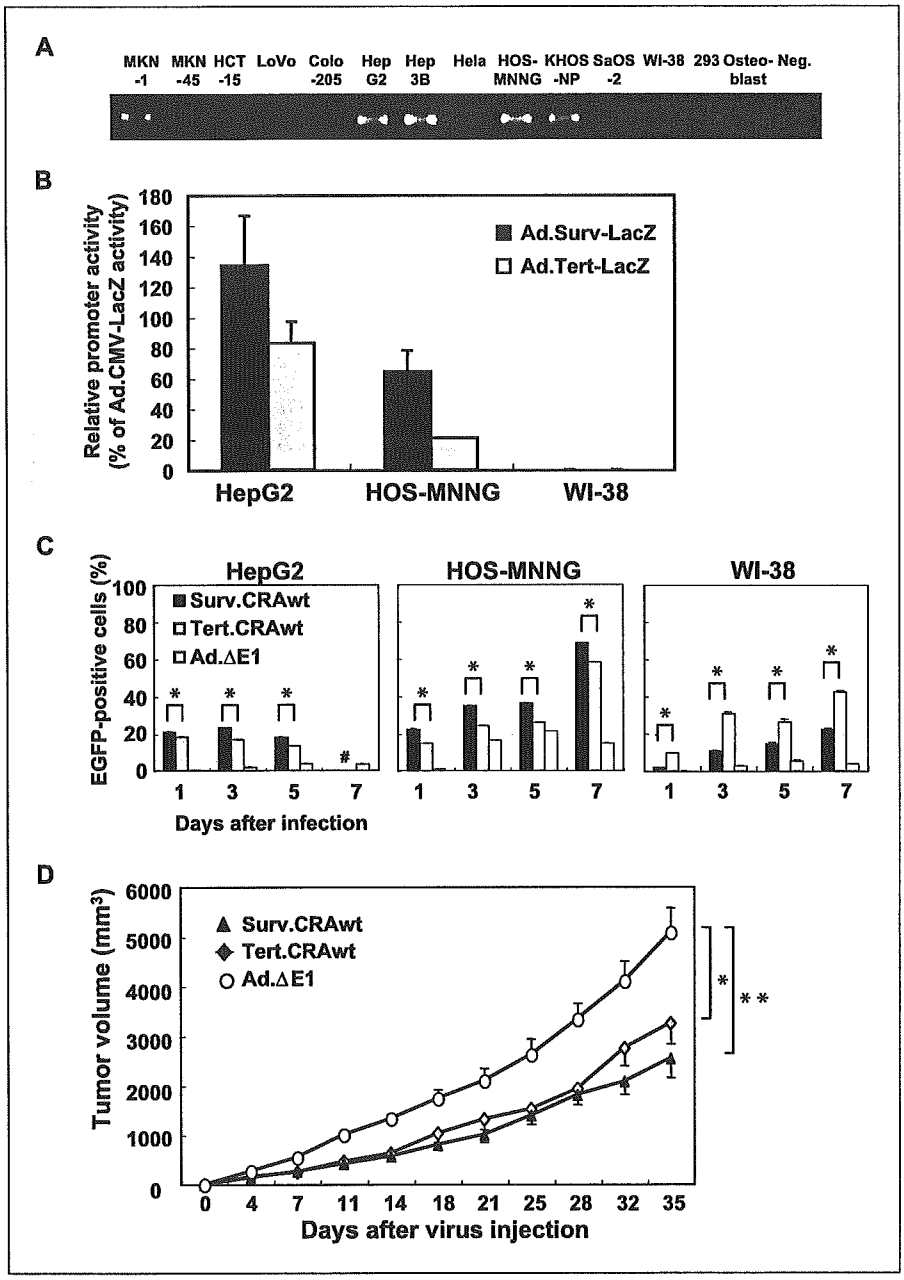

Figure 6. Comparison of Surv.CRA with Tert.CRA. *A*, endogenous TERT mRNA was detected by RT-PCR. *B*, relative activity of the *survivin* promoter and the TERT promoter to that of the CMV promoter. X-gal activity was determined 48 hours after infection with Ad.Surv-LacZ, Ad.Tert-LacZ, or Ad.CMV-LacZ at an MOI of 30. *C*, rate of viral propagation was assessed by flow cytometric analysis, expressed as the percentage of EGFP-positive cells 1, 3, 5, and 7 days after infection with either adenoviruses at an MOI of 0.03 in HepG2 cells and an MOI of 0.1 in HOS-MNNG and WI-38 cells. *, $P < 0.05$. Both Surv.CRAwt and Tert.CRAwt rapidly replicated between 5 and 7 days after infection of HepG2 cells at this MOI; infected cells detached from the culture dishes at seven days post infection (#). *D*, tumor volume was measured after a single injection of 1×10^8 pfu Surv.CRAwt ($n = 8$), Tert.CRAwt ($n = 9$), or control Ad.ΔE1 ($n = 11$) into preestablished s.c. HOS-MNNG tumors in nude mice. *, $P < 0.05$ and **, $P < 0.005$ (statistical significance in comparison with control Ad.ΔE1).

phenotypes, including low levels of *survivin* expression. The problem of low AGTE in certain cancer types is a critical issue in adenoviral gene therapy; Surv.CRAs are no exception. Further attempts should be made to improve adenoviral infectivity. Nevertheless, this study showed that Surv.CRAs propagated even in cell types with low AGTE values, a promising result for the potential of these vectors as therapeutic agents. In addition, we intentionally used HOS-MNNG cells, which express *survivin* at relatively low levels and exhibit only moderate AGTE, for *in vivo* animal studies. The anticancer effect of Surv.CRAs under these conditions suggests that this agent may elicit therapeutic effects in many cancer types. Moreover, recent studies have detailed promising approaches to overcome the obstacle of low AGTE, such as fiber modification (31–33); these techniques could be also be directly and feasibly applied to Surv.CRAs (22). Fiber-modified Surv.CRA may enhance the cancer specificity and efficacy of this therapy for a broader range of cancer types and should be explored further.

Another crucial requirement for optimal CRA is attenuation of viral replication in normal cells. Currently, one of the best available CRAs may be Tert.CRA; TERT, the major determinant of telomerase activity, is expressed at high levels in many cancer cells but not in normal cells (34). Several recent studies have shown cancer-selective replication and anticancer effects of Tert.CRAs (18–20). After examining the endogenous expression levels and promoter activity of TERT in a variety of cancer and normal cells, we compared the viral replication of Surv.CRAwt to that of Tert.CRAwt in both cancer and normal cells. Surv.CRAwt showed greater promise; the replication of Surv.CRAs in normal cells was more

attenuated than that of the Tert.CRA, whereas Surv.CRAwt was more efficient in replicating in two independent cancer cell types, including HOS-MNNG. As HOS-MNNG expressed *survivin* and TERT at low and high levels, respectively, it is likely that Surv.CRAs are superior to Tert.CRAs in both cancer specificity and efficiency, although the general applicability of this trend will need to be confirmed in future studies.

Previous studies have not yet explored whether deletion of the RB-binding domain when combined with the modulation of E1A expression using a tumor-specific promoter provides additional advantages or disadvantages over either approach alone (4). In this study, Surv.CRAmt did not provide an enhanced cancer specificity or an attenuation of viral replication in normal cells but also do not reduce viral replication in the cancer cells examined, including both RB-deficient and RB-intact tumor cells and normal fibroblast cells. The *survivin* promoter may confer such a high level of cancer specificity that these additional viral modifications do not provide a clear additional advantage. It is also possible that both RB-dependent and *survivin*-dependent cancer specificities target cell cycle dysregulation; therefore, the cancer specificity of RB- and *survivin*-dependent viruses may overlap to some extent. Future studies should be conducted to modify further the expression elements of other adenoviral genes using different promoters that target cancer-specific genetic events independent of cell cycle dysregulation, because the replication of Surv.CRAs in normal cells was greatly attenuated but not completely abrogated.

In conclusion, this study showed the therapeutic potential of *survivin*-responsive CRAs; these Surv.CRAs confer cancer-specific replication and cytotoxicity and thus may provide an attractive therapeutic agent for the treatment of cancer.

Acknowledgments

Received 7/26/2004; revised 3/30/2005; accepted 4/12/2005.

Grant support: A Grant-in-Aid for Scientific Research on Priority Areas (C); a grant for Cooperation of Innovative Technology and Advanced Research in Evolutional Area from the Ministry of Education, Culture, Sports, Science and Technology, Japan; and Health and Labour Sciences Research Grants for Third Term Comprehensive Control Research for Cancer from the Ministry of Health, Labour and Welfare, Japan.

The costs of publication of this article were defrayed in part by the payment of page charges. This article must therefore be hereby marked *advertisement* in accordance with 18 U.S.C. Section 1734 solely to indicate this fact.

We thank M. Saito and A. Kusano for their technical assistance, Dr. S. Kyo for providing the material, and David Cochran for editing the article.

References

1. Alemany R, Balague C, Curiel DT. Replicative adenoviruses for cancer therapy. Nat Biotechnol 2000;18:723–7.
2. Fueyo J, Gomez-Manzano C, Alemany R, et al. A mutant oncolytic adenovirus targeting the Rb pathway produces anti-glioma effect *in vivo*. Oncogene 2000; 19:2–12.
3. Bischoff JR, Kirn DH, Williams A, et al. An adenovirus mutant that replicates selectively in p53-deficient human tumor cells. Science 1996;274:373–6.
4. Heise C, Hermiston T, Johnson L, et al. An adenovirus E1A mutant that demonstrates potent and selective systemic anti-tumoral efficacy. Nat Med 2000;6:1134–9.
5. Rothmann T, Hengstermann A, Whitaker NJ, Scheffner M, zur Hausen H. Replication of ONYX-015, a potential anticancer adenovirus, is independent of p53 status in tumor cells. J Virol 1998;72:9470–8.
6. Harada JN, Berk AJ. p53-Independent and -dependent requirements for E1B-55K in adenovirus type 5 replication. J Virol 1999;73:5333–44.
7. Rodriguez R, Schuur ER, Lim HY, Henderson GA, Simons JW, Henderson DR. Prostate attenuated replication competent adenovirus (ARCA) CN706: a selective cytotoxic for prostate-specific antigen-positive prostate cancer cells. Cancer Res 1997;57:2559–63.
8. Hallenbeck PL, Chang YN, Hay C, et al. A novel tumor-specific replication-restricted adenoviral vector for gene therapy of hepatocellular carcinoma. Hum Gene Ther 1999;10:1721–33.
9. Adachi Y, Reynolds PN, Yamamoto M, et al. A midkine promoter-based conditionally replicative adenovirus for treatment of pediatric solid tumors and bone marrow tumor purging. Cancer Res 2001;61:7882–8.
10. Nettelbeck DM, Rivera AA, Balague C, Alemany R, Curiel DT. Novel oncolytic adenoviruses targeted to melanoma: specific viral replication and cytolysis by expression of E1A mutants from the tyrosinase enhancer/promoter. Cancer Res 2002;62:4663–70.
11. Ambrosini G, Adida C, Altieri DC. A novel anti-apoptosis gene, survivin, expressed in cancer and lymphoma. Nat Med 1997;3:917–21.
12. Altieri DC. The molecular basis and potential role of survivin in cancer diagnosis and therapy. Trends Mol Med 2001;7:542–7.
13. Li F, Ambrosini G, Chu EY, et al. Control of apoptosis and mitotic spindle checkpoint by survivin. Nature 1998;396:580–4.
14. Bao R, Connolly DC, Murphy M, et al. Activation of cancer-specific gene expression by the survivin promoter. J Natl Cancer Inst 2002;94:522–8.
15. Li F, Altieri DC. The cancer antiapoptosis mouse survivin gene: characterization of locus and transcriptional requirements of basal and cell cycle-dependent expression. Cancer Res 1999;59:3143–51.
16. Li F, Altieri DC. Transcriptional analysis of human survivin gene expression. Biochem J 1999;344 Pt 2:305–11.
17. Zwicker J, Lucibello FC, Wolfraim LA, et al. Cell cycle regulation of the cyclin A, cdc25C and cdc2 genes is based on a common mechanism of transcriptional repression. EMBO J 1995;14:4514–22.
18. Huang TG, Savontaus MJ, Shinozaki K, Sauter BV, Woo SL. Telomerase-dependent oncolytic adenovirus for cancer treatment. Gene Ther 2003;10:1241–7.
19. Wirth T, Zender L, Schulte B, et al. A telomerase-dependent conditionally replicating adenovirus for selective treatment of cancer. Cancer Res 2003;63: 3181–8.
20. Kim E, Kim JH, Shin HY, et al. Ad-mTERT-δ19, a conditional replication-competent adenovirus driven by the human telomerase promoter, selectively replicates in and elicits cytopathic effect in a cancer cell-specific manner. Hum Gene Ther 2003;14: 1415–28.
21. Takakura M, Kyo S, Kanaya T, et al. Cloning of human telomerase catalytic subunit (hTERT) gene promoter and identification of proximal core promoter sequences essential for transcriptional activation in immortalized and cancer cells. Cancer Res 1999;59:551–7.
22. Nagano S, Oshika H, Fujiwara H, Komiya S, Kosai K. An efficient construction of conditionally replicating adenoviruses that target tumor cells with multiple factors. Gene Ther. In press 2005.
23. Chen SH, Chen XH, Wang Y, et al. Combination gene therapy for liver metastasis of colon carcinoma *in vivo*. Proc Natl Acad Sci U S A 1995;92:2577–81.
24. Kawai T, Takahashi T, Esaki M, et al. Efficient cardiomyogenic differentiation of embryonic stem cell by fibroblast growth factor 2 and bone morphogenetic protein 2. Circ J 2004;68:691–702.
25. Yan P, Coindre JM, Benhattar J, Bosman FT, Guillou L. Telomerase activity and human telomerase reverse transcriptase mRNA expression in soft tissue tumors: correlation with grade, histology, and proliferative activity. Cancer Res 1999;59:3166–70.
26. Melton DW, Konecki DS, Brennand J, Caskey CT. Structure, expression, and mutation of the hypoxanthine phosphoribosyltransferase gene. Proc Natl Acad Sci U S A 1984;81:2147–51.
27. Terazaki Y, Yano S, Yuge K, et al. An optimal therapeutic expression level is crucial for suicide gene therapy for hepatic metastatic cancer in mice. Hepatology 2003;37:155–63.
28. Fukunaga M, Takamori S, Hayashi A, Shirouzu K, Kosai K. Adenoviral herpes simplex virus thymidine kinase gene therapy in an orthotopic lung cancer model. Ann Thorac Surg 2002;73:1740–6.
29. Nagano S, Yuge K, Fukunaga M, et al. Gene therapy eradicating distant disseminated micro-metastases by optimal cytokine expression in the primary lesion only: novel concepts for successful cytokine gene therapy. Int J Oncol 2004;24:549–58.
30. Bonnekoh B, Greenhalgh DA, Bundman DS, et al. Adenoviral-mediated herpes simplex virus-thymidine kinase gene transfer *in vivo* for treatment of experimental human melanoma. J Invest Dermatol 1996; 106:1163–8.
31. Kawakami Y, Li H, Lam JT, Krasnykh V, Curiel DT, Blackwell JL. Substitution of the adenovirus Serotype 5 Knob with a Serotype 3 Knob enhances multiple steps in virus replication. Cancer Res 2003;63: 1262–9.
32. Davydova J, Le LP, Gavrikova T, Wang M, Krasnykh V, Yamamoto M. Infectivity-enhanced cyclooxygenase-2-based conditionally replicative adenoviruses for esophageal adenocarcinoma treatment. Cancer Res 2004;64: 4319–27.
33. Liu Y, Ye T, Sun D, Maynard J, Deisseroth A. Conditionally replication-competent adenoviral vectors with enhanced infectivity for use in gene therapy of melanoma. Hum Gene Ther 2004;15:637–47.
34. Ito H, Kyo S, Kanaya T, Takakura M, Inoue M, Namiki M. Expression of human telomerase subunits and correlation with telomerase activity in urothelial cancer. Clin Cancer Res 1998;4:1603–8.

Gene Therapy (2005), 1–9

www.nature.com/gt

RESEARCH ARTICLE

An efficient construction of conditionally replicating adenoviruses that target tumor cells with multiple factors

S Nagano[1,2,3], H Oshika[4], H Fujiwara[5], S Komiya[2] and K Kosai[1,3,4]

[1]Division of Gene Therapy and Regenerative Medicine, Cognitive and Molecular Research Institute of Brain Diseases, Kurume University, Kurume, Japan; [2]Department of Orthopaedic Surgery, Graduate School of Medical and Dental Sciences, Kagoshima University, Kagoshima, Japan; [3]Department of Pediatrics and Child Health, Kurume University School of Medicine, Kurume, Japan; [4]Department of Gene Therapy and Regenerative Medicine, Gifu University School of Medicine, Gifu, Japan; and [5]Department of Cardiology, Respiratory and Nephrology, Regeneration & Advanced Medical Science, Graduate School of Medicine, Gifu University, Gifu, Japan

Despite the enormous potential of conditionally replicating adenoviruses (CRAs), the time-consuming and laborious methods required to construct CRAs have hampered both the development of CRAs that can specifically target tumors with multiple factors (m-CRA) and the efficient analysis of diverse candidate CRAs. Here, we present a novel method for efficiently constructing diverse m-CRAs. Elements involving viral replication, therapeutic genes, and adenoviral backbones were separately introduced into three plasmids of P1, P2, and P3, respectively, which comprised different antibiotic resistant genes, different ori, and a single loxP (H) sequence. Independently constructed plasmids were combined at 100% accuracy by transformation with originally prepared Cre and specific antibiotics in specific Escherichia coli; transfection of the resulting P1+2+3 plasmids into 293 cells efficiently generated m-CRAs. Moreover, the simultaneous generation of diverse m-CRAs was achieved at 100% accuracy by handling diverse types of P1+2 and P3. Alternatively, co-transfection of P1+3 and P2 plasmids into Cre-expressing 293 cells directly generated m-CRA with therapeutic genes. Thus, our three-plasmid system, which allows unrestricted construction and efficient fusion of individual elements, should expedite the process of generating, modifying, and testing diverse m-CRAs for the development of the ideal m-CRA for tumor therapy.

Gene Therapy advance online publication, 5 May 2005; doi:10.1038/sj.gt.3302540

Keywords: *conditionally replicating adenovirus; cancer; tumor-specific; Cre/lox recombination*

Introduction

One of the major obstacles to cancer gene therapy is inefficient and nonspecific gene delivery to cancer cells, leading to unsatisfactory outcomes in clinical trials due to recurrence from nontransduced tumor cells, even though some of the effective strategies, such as suicide gene therapy,[1,2] immunological gene therapy,[3,4] and their combinations[5] may treat nontransduced tumor cells to some degree and partially circumvent this problem. Conditionally replicating adenoviruses (CRAs), which selectively replicate in tumor cells, but not in normal cells, have the potential to circumvent this problem and to achieve tumor-specific gene delivery.[6,7] Moreover, CRA itself may be an attractive tool for innovative cancer therapy because selectively propagated adenovirus (Ad) induces the lysis of tumor cells. While various CRAs have been reported to date, the majority of them may be classified into two groups.[8] One is CRA that expresses E1 in a tumor-specific manner by the replacement of a native E1 promoter with various tumor-specific promoters.[9–12] The other is CRA with a partial deletion of the *E1* gene; the representatives are the mutant (mt) type of Ad lacking a p53-binding protein that is encoded by E1B55kD (ONYX-015),[13] and the mt Ad lacking an Rb-binding site of E1A (Δ24).[14,15] In the case of infection with the wild type of Ad, E1B55kD inhibits the p53-induced apoptosis of the host cell and enables Ad to continuously replicate in cells.[13,16] In addition, the interaction of adenoviral E1A with cellular Rb leads to the release of E2F transcription factor, which induces S-phase transition of the host cell in order to facilitate viral replication.[16] Based on these theories, neither mt ONYX-015 nor Δ24 may efficiently replicate in normal cells with intact Rb and p53, whereas both CRAs may actively replicate in the majority of tumor cells, disrupting the Rb-E2F pathway and/or p53 function.

However, a perfect CRA, which replicates efficiently in cancer cells but is completely attenuated in normal cells, has not yet been established in reality. Especially, the crucial problem of current CRAs is the insufficient or incomplete cancer specificity; that is, these CRAs do replicate in and cause some cytopathic effects, while greatly attenuated, in normal cells.[17–19] Recent studies suggested that CRAs with two or three tumor specific

Correspondence: Dr K Kosai, Division of Gene Therapy and Regenerative Medicine, Cognitive and Molecular Research Institute of Brain Diseases, Kurume University, 67 Asahi-machi, Kurume, Fukuoka, 830-0011, Japan
Received 2 November 2004; accepted 28 February 2005

factors enhanced their tumor specificity: mt E1A and mt E1B,[20] two tumor-specific promoters,[21] or a tumor-specific promoter and mt E1A.[12,22] In this regard, a promising approach to circumvent this obstacle might be combining and introducing multiple (more than three) tumor-specific factors into a single CRA. However, extensive and comparative studies on CRAs that are regulated with multiple tumor-specific factors (m-CRAs) are currently hampered by the lack of standardized methods to efficiently construct m-CRAs in contrast to well-established methods for efficiently constructing E1-deleted replication-incompetent Ad vectors.[23–25] It remains time-consuming and laborious to construct diverse m-CRAs using current methods; the requirement of additional modification steps hampers efficient production of diverse m-CRAs in large numbers by the same protocol. In addition, although functions of individual viral proteins have been largely elucidated,[16] the controversy over p53-dependent replication of the most representative CRA, ONYX-015,[13,17,18] suggests the necessity of extensive biological and systematic virological analyses of a large number of diverse m-CRAs in practice.

Here, we develop a novel method for the efficient construction of m-CRAs; this system simplifies and expedites the generation and modification of m-CRAs.

Results

Constitution of m-CRAs

One of the characteristic features of our method is the independent and unrestricted construction of three different regulatory elements in m-CRA, involving viral replication, therapeutic genes, and Ad backbones. To this end, these elements were separately introduced into three plasmids (Figure 1a). Replication-controllable plasmid P1 consists of wt or mt E1A and E1B sequences. Therapeutic gene-cloning plasmid P2 characteristically contains the tetracycline resistance gene (*tet*^{r}) and *R6Kγ ori*, which render this plasmid selectively amplified in only a specific type of *Escherichia coli* (*E. coli*) expressing the *pir* gene.[26] The Ad backbone plasmid P3 was described previously.[23] Potentially, more than seven tumor-specific factors can be introduced into the m-CRA (Figure 1a).

The use of different antibiotic resistance genes in all three plasmids, characteristically specific *ori* in P2 and unique I-*Ceu*I and PI-*Sce*I restriction sites in P1 and P3, enable the independent and unrestricted construction of three plasmids, and, subsequently, the feasible and rapid fusion of these three plasmids to generate a single CRA plasmid without using a regular ligation procedure. This is accomplished in the following manner (Figure 1b). Four variants of P1 vector with different combinations of wt or mt of E1A and E1B can be chosen at present. After the therapeutic gene and the promoters of interest were inserted into the multiple-cloning sites in P1 and P2, these two vectors were mixed and incubated with *Cre* aliquot. DH5α *E. coli* was transformed using all of the mixtures, and then grown on LB plates containing 5 μg/ml tetracycline. As P1 or P2 has either the kanamycin resistance gene (*kan*^{r}) or *R6Kγ ori* but not both, only the DH5α clone containing successfully recombined plasmid P1+2 will grow and form a colony on the LB plates containing tetracycline. P3 is digested with I-*Ceu*I and PI-*Sce*I, and ligated with I-*Ceu*I/PI-*Sce*I-digested P1+2, yielding a single P1+2+3 plasmid. Finally, this P1+2+3 plasmid, that is, Ad vector plasmid containing a replication-regulatory element and therapeutic gene, is linearized by *Pac*I, and transfected into 293 cells, as described previously.[5,23] Miniprep DNA can be used in all of the procedures, including the transfection; this feature increases the rapidity of this method and allows the handling of numerous samples simultaneously.

Preparation of Cre recombinase

Commercial *Cre* recombinase is so expensive that it prohibits the manipulation of a large number of samples in the present system. To circumvent this obstacle, we developed a feasible and inexpensive way to obtain a solution containing highly active *Cre* recombinase as follows. HepG2 cells, which demonstrated the highest level of transgene expression and the highest adenoviral gene transduction efficiency (data shown elsewhere), were infected with Ad.CA-Cre (Ad expressing Cre under the strongest CA promoter, which was kindly donated by I Saito) at an MOI of 30 for 2 days, and were then harvested and lysed in 200 μl buffer containing 20 mM Tris-HCl pH 7.5, 150 mM NaCl, 1 mM EDTA, and 10% glycerol by three rounds of freeze–thawing. The supernatants after centrifugation were collected and stored in aliquots at −80°C until use.

We compared the activity of our *Cre* aliquot with commercial products using two plasmids which had a single loxP sequence. At 1 day after the transformation of *E. coli* with our *Cre* aliquot and growth on 10 cm LB plates, several hundred colonies appeared and all colonies were correctly recombined to form a single plasmid (data not shown). Unexpectedly, two of the three commercial lots from two representative companies did not work well (no and one colony). Thus, the *Cre* activity in our aliquot was sufficiently high for reliable *Cre/lox* recombination in *E. coli*; we used this *Cre* aliquot for the following m-CRA construction (supernatant from one 10 cm dish allowed 200 samples of reaction).

Construction of CEA-responsive m-CRAs

To test the efficiency and the feasibility of this system, we generated carcinoembryonic antigen (CEA) responsive m-CRAs as an example, in which either wt or mt E1A was expressed under the transcriptional control of the CEA promoter (CEApr). Both types of m-CRA have mt E1B (E1BΔ55kD) downstream from the cytomegalovirus immediate-early gene enhancer/promoter (CMVpr). As a P2 plasmid, pUni/CMVpr-EGFP was used.

After the recombination of P1 and P2 with *Cre* aliquot, followed by the transformation of DH5α and growth, 10–50 colonies per 10 cm LB-tetracycline plate appeared. Notably, restriction enzyme analyses demonstrated that all of the clones contained the correctly recombined plasmid (pCEApr-E1A-CMVpr-E1BΔ55kD/CMVpr-EGFP or pCEApr-E1AΔ24–CMVpr-E1BΔ55kD/CMVpr-EGFP; we term each P1+2 plasmid as 'pP1-component/P2-component') (Figure 2a). The somewhat lower titer here than that shown in an earlier section was due to tetracycline selection, but not due to *Cre/lox* recombination efficiency, according to our preliminary studies (data not shown), whereas the result of 100% accuracy in 10–50

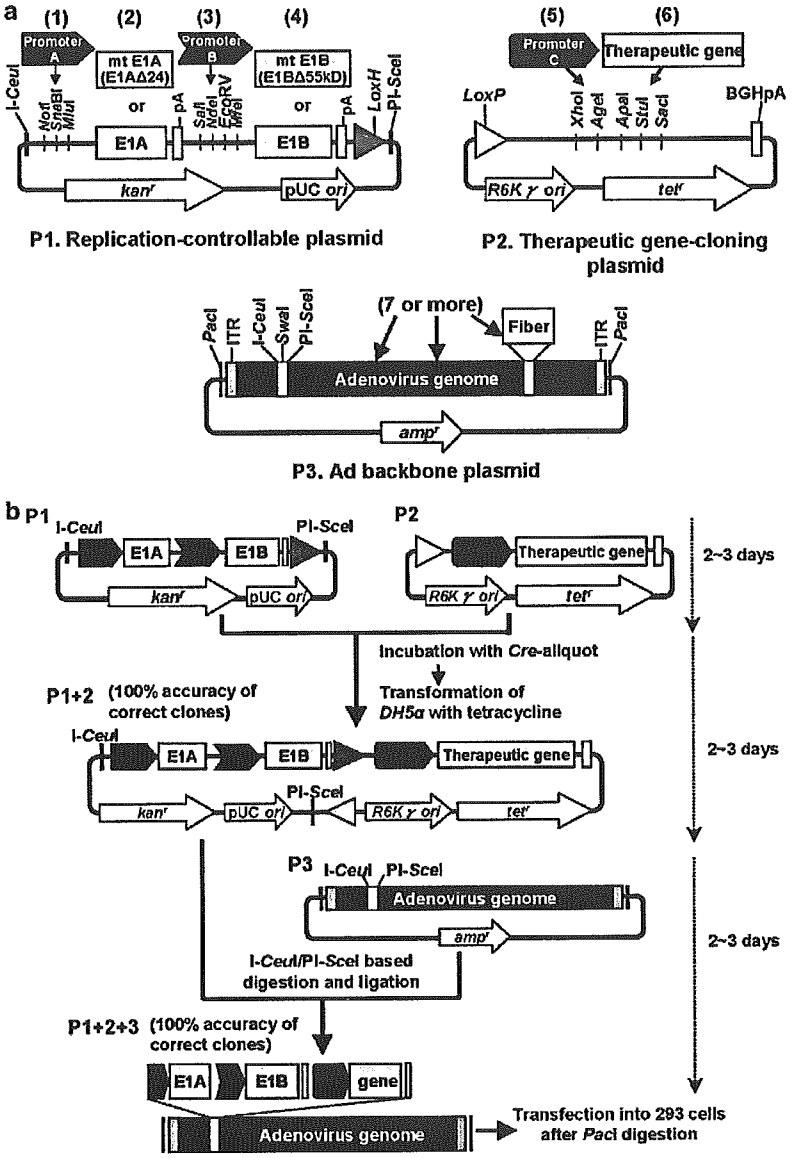

Figure 1 *The constitution and construction of m-CRA. (a) The constitution of the vector plasmids. Potentially, more than seven tumor-specific factors can be introduced into the m-CRA as follows. (1) Promoter A, which drives wt or mt E1A. (2) mt E1A, which lacks an Rb-binding site (E1AΔ24). (3) Promoter B, which drives wt or mt E1B. (4) mt E1B, which lacks a p53-binding protein that is encoded by E1B55kD (E1BΔ55kD). (5) Promoter C, which drives a therapeutic gene. (6) A therapeutic gene. (7 or more) Modification of Ad backbone, such as a fiber modification to modulate an infectivity. (b) The schematic representation of the m-CRA construction. All procedures, including the transfection into 293 cells, can be carried out using miniprep DNA.*

colonies was rather encouraging and sufficient for the present purpose.

Elements involving viral replication and the therapeutic gene were transferred from P1+2 to P3 (pAd.HM4) to generate P1+2+3 (pAd.HM4-CEApr-E1A-CMVpr-E1BΔ55kD/CMVpr-EGFP or pAd.HM4-CEApr-E1AΔ24–CMVpr-E1BΔ55kD/CMVpr-EGFP; we term each P1+2+3 adenoviral plasmid as 'pAd.P3-component-P1-component/P2-component'). The accuracy of such unique I-*Ceu*I/PI-*Sce*I-based ligation was almost 100% (Figure 2b), in accordance with the previous results.[23] Over 10 plaques appeared on 6 cm dishes 12 days after the transfection of *Pac*I-digested P1+2+3 into 293 cells. Notably, all of the plaques were EGFP-positive under fluorescent microscopy (Figure 2c). Accordingly, the PCR analyses of the DNA extracted from these m-CRAs verified that all of them were correct CEA-responsive m-CRA (CRA.CEApr-E1A-CMVpr-E1BΔ55kD/CMVpr-EGFP or CRA.CEApr-E1AΔ24-CMVpr-E1BΔ55kD/CMVpr-EGFP; we term each m-CRA as 'CRA.P1-component/P2-component') (Figure 2d).

Simultaneous construction of diverse types of m-CRAs

It would further facilitate extensive analyses of m-CRAs if numerous and diverse types of m-CRAs could be constructed at one time. To investigate this possibility, we first investigated whether initially constructed P1+3, that is, Ad backbone plasmid with a replication-regulatory

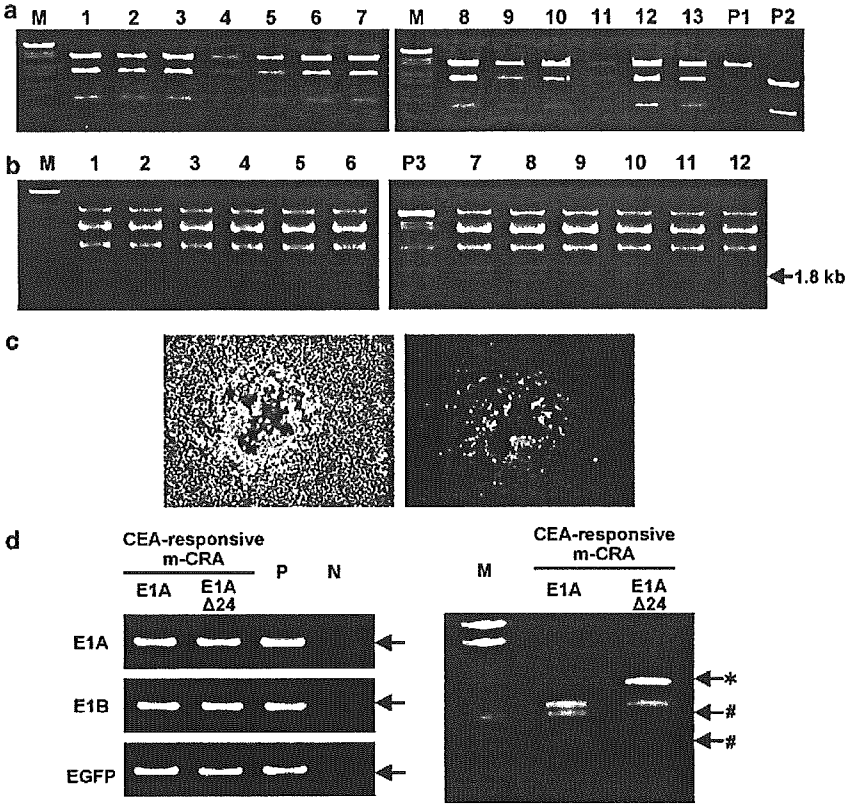

Figure 2 The efficiency and accuracy in the m-CRA construction on the protocol shown in Figure 1b. (a) Restriction enzyme analysis of P1+2 plasmid. After the reaction of pCEApr-E1A-CMVpr-E1BΔ55kD (P1) and pUni-CMVpr-EGFP (P2), 13 miniprep samples from E. coli colonies were digested by SalI and electrophoresed (M, marker. Lanes 1–13, each sample; P1, P1 plasmid; P2, P2 plasmid). The correct pattern (three bands consisting of P1-derived 6.3 kb band and P2-derived 3.2 and 1.2 kb bands) was seen in all samples, demonstrating 100% accuracy of correct clones containing P1+2 plasmid (pCEApr-E1A-CMVpr-E1BΔ55kD/CMVpr-EGFP) among all of the transformed clones. (b) Restriction enzyme analysis of P1+2+3 plasmid. After the reaction of P1+2 (pCEApr-E1A-CMVpr-E1BΔ55kD/CMVpr-EGFP) and P3 (pAd.HM4), 12 miniprep samples from E. coli colonies were digested with HindIII and electrophoresed (M, marker. Lanes 1–12, each sample; P3, P3 plasmid). The correct pattern was seen in all samples; the 1.8 kb band was indicative of the correct clone. (c) Phase-contrast (left) and fluorescent (right) microscopic pictures of one representative of m-CRA plaques (CRA.CEApr-E1A-CMVpr-E1BΔ55kD/CMVpr-EGFP) on 293 cells 10 days after transfection of PacI-digested pAd.HM4-CEApr-E1A-CMVpr-E1BΔ55kD/CMVpr-EGFP. (d) PCR analyses of genomic DNA extracted from m-CRA plaques. PCR was performed with three different primer sets of S-E1A-1/AS-E1A-1, S-E1B-1/AS-E1B-1, and S-EGFP/AS-EGFP to detect E1A, E1A, and EGFP DNA, respectively, in CEA-responsive m-CRAs (E1A; CRA.CEApr-E1A-CMVpr-E1BΔ55KD/CMVpr-EGFP, and E1AΔ24; CRA.CEApr-E1AΔ24-CMVpr-E1BΔ55kD/CMVpr-EGFP) (the left picture). P, positive control plasmid DNA corresponding to each of primer sets. N, nontemplate DNA. To distinguish these two CEA-responsive m-CRAs, PCR products amplified with the primer sets of S-HM5 and AS-E1A-1 were digested with BstXI, of which recognition sites existed in the Rb-binding domain of E1A and Ad backbone (the right picture). The correct pattern was seen in all samples of both types of m-CRA; the 0.8 kb band (*), and the 0.5 and 0.3 kb bands (#) were indicative of m-CRA with mt E1A (E1AΔ24), and that with wtE1A, respectively.

element, might be recombined with therapeutic gene-cloning vector P2 in the same way as the recombination of P1 and P2 (Figure 3a). P1+3 (pAd.HM4-CEApr-E1A-CMVpr-E1BΔ55kD) was constructed by transferring replication-regulatory elements from P1 (pCEApr-E1A-CMVpr-E1BΔ55kD) to P3 (pAd.HM4) with I-*Ceu*I/PI-*Sce*I-based ligation. After incubating P1+3 (pAd.HM4-CEApr-E1A-CMVpr-E1BΔ55kD) and P2 (pUni/CMVpr-EGFP) with *Cre* aliquot, DH5α was transformed with all of the mixtures and grew on LB plates with tetracycline. After 1 day, about 30 colonies appeared on a 10 cm dish, and all of them contained correctly recombined P1+2+3 plasmid (pAd.HM4-CEApr-E1A-CMVpr-E1BΔ55kD/CMVpr-EGFP) (Figure 3b). Thus, both the efficiency and accuracy of the recombination/transformation of P1+2 and P3 were similarly high in comparison with those of P1 and P2, as shown in the earlier section, although P1+3 was a much larger plasmid than P1 alone.

Next, the feasibility of simultaneously constructing several different types of m-CRAs was tested. DH5α *E. coli* in each of 10 tubes containing the same P2 (pUni/CMVpr-EGFP) and *Cre* aliquot was transformed by each of 10 different types of P1+3 plasmid. At 1 day after the growth on LB-tetracycline plates, 3–52 colonies appeared on each of the 10 cm plates, and all colonies were correctly recombined plasmids (Figure 3c).

Furthermore, we examined whether more different tumor-specific factors including therapeutic genes can be correctly inserted into m-CRAs with the present system. Eight different m-CRAs that contain six tumor-specific factors, that is, (1) human telomerase reverse transcriptase promoter (TERTpr) driving E1A, (2) wt or mt E1A, (3) human E2F promoter (E2Fpr) driving E1B, (4) mt E1B,

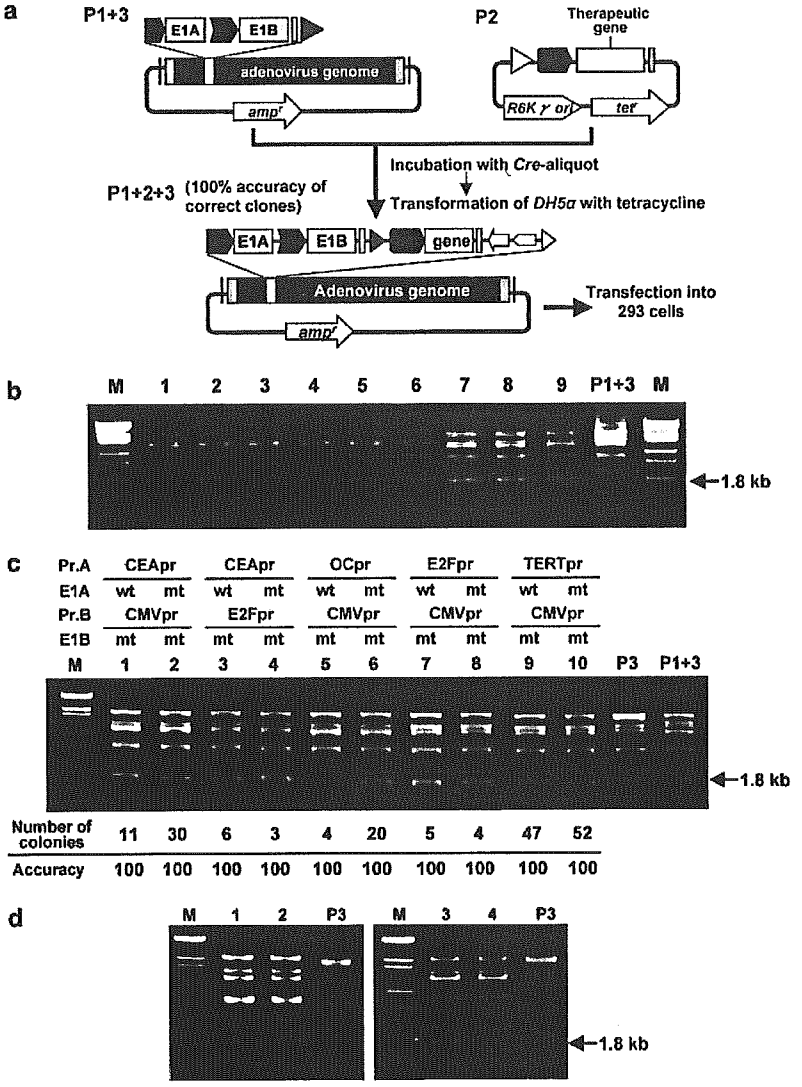

Figure 3 Simultaneous construction of diverse types of m-CRA plasmids. (a) The schematic representation. Initially constructed P1+3, that is, Ad backbone plasmid with a replication-regulatory element, can be recombined with therapeutic gene-cloning vector P2 to yield a single P1+2+3 plasmid. (b) Restriction enzyme analysis of genomic DNA extracted from clones transformed with P1+3 (pAd.HM4-CEApr-E1A-CMVpr-E1BΔ55kD) and P2 (pUni/CMVpr-EGFP). HindIII digestion of miniprep samples demonstrated the correct pattern of P1+2+3 plasmid (pAd.HM4-CEApr-E1A-CMVpr-E1BΔ55kD/CMVpr-EGFP) in all of the transformed clones (M, marker. Lanes 1–9, each sample; P1+3, P1+3 plasmid); the 1.8 kb band was indicative of the correct clone. (c, d) Simultaneous construction of several different types of m-CRAs with this protocol. (c) DH5α E. coli in each of 10 tubes containing the same P2 (pUni/CMVpr-EGFP) and each of 10 different types of P1+3 plasmid, which were preincubated with the Cre aliquot, were transformed and grew with tetracycline. HindIII-digestion analysis was carried out in the same manner as above, and one representative picture per group was shown here. Numbers of colonies per 10 cm plate appeared and the accuracy (the percentage of the correct clones; clones in each group were carefully analyzed with several different types of restriction enzymes although data were not shown here) in each group is shown below the picture (M, marker. Lanes 1–10, each sample; Pr.A, promoter driving wt or mt E1A; Pr.B, promoter driving wt or mt E1B; P3, P3 plasmid; P1+3, P1+3 plasmid). The 1.8 kb band was indicative of the correct clone. (d) Four different CRAs which contain six tumor-specific factors were constructed and the P1+2+3 plasmids were analyzed by HindIII digestion (M, marker. Lane 1, pAd.HM4-TERTpr-E1A-E2Fpr-E1BΔ55kD/Surv.pr-p53; Lane 2, pAd.HM4-TERTpr-E1AΔ24-E2Fpr-E1BΔ55kD/Surv.pr-p53; Lane 3, pAd.HM12-TERTpr-E1A-E2Fpr-E1BΔ55kD/Surv.pr-tk; each sample; Lane 4, pAd.HM12-TERTpr-E1AΔ24-E2Fpr-E1BΔ55kD/Surv.pr-tk; P3, P3 plasmid).

(5) mouse survivin promoter (Surv.pr) or CMVpr driving therapeutic gene, and (6) therapeutic gene (p53 or herpes simplex virus thymidine kinase (HSV-tk), were successfully constructed (Figure 3d and data not shown).

Thus, it was shown that simultaneous construction of diverse m-CRAs was, in fact, feasible using the present system.

Therapeutic gene insertion into m-CRA directly in Cre-expressing 293 cells (alternative protocol)

We further hypothesized that two types of plasmids, P1+3 and P2, might be recombined directly in *Cre*-expressing 293 cells (Figure 4a). To assess this possibility, P1+3 (pAd.HM4-CEApr-E1A-CMVpr-E1BΔ55kD) and

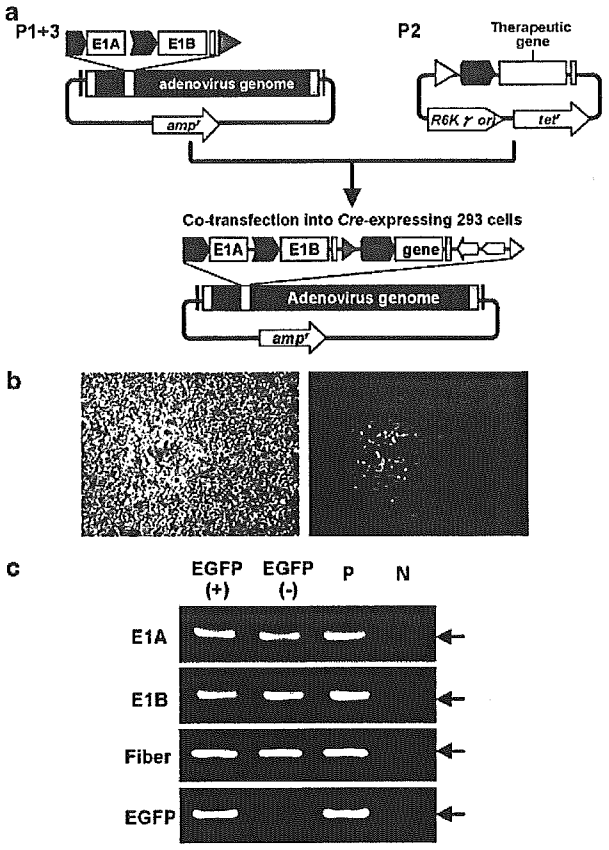

Figure 4 Therapeutic gene insertion into m-CRA directly in Cre-expressing 293 cells (alternative protocol). (a) The schematic representation. (b) Phase-contrast (left) and fluorescent (right) microscopic pictures of an m-CRA plaque (CRA.CEApr-E1A-CMVpr-E1BΔ55kD/CMVpr-EGFP) on Cre-expressing 293 cells 12 days after co-transfection of P1+3 (pAd.HM4-CEApr-E1A-CMVpr-E1BΔ55kD) and P2 (pUni/CMVpr-EGFP). (c) PCR analyses of genomic DNA extracted from m-CRA plaques that do or do not show EGFP fluorescence (two left lanes, respectively). PCR analyses were performed using four different primer sets of S-E1A-1/AS-E1A-1, S-E1B-1/AS-E1B-1, S-Fiber/AS-Fiber, and S-EGFP/AS-EGFP to detect E1A, E1B, fiber, and EGFP DNA, respectively. P, positive control plasmid DNA corresponding to each of primer sets. N, nontemplate DNA.

P2 (pUni/CMVpr-EGFP) were cotransfected into *Cre*-expressing 293 cells. Some plaques became visible 6 days afterwards, and 10 plaques per 10 cm dish appeared 12 days after cotransfection. One of these 10 plaques showed an EGFP-positive finding under fluorescent microscopy (Figure 4b). PCR analysis of the DNA isolated from these plaques verified that only this fluorescence-positive plaque contained a correctly recombined m-CRA with EGFP cDNA (Figure 4c). Therefore, using a marker gene such as *EGFP*, the correct m-CRA derived from P1+2+3 plasmid can be easily isolated from the m-CRA derived from P1+3 plasmid.

Discussion

The large size of the adenoviral DNA (36 kB) hampered the feasible modification of the Ad vector, due to limited numbers of available unique restriction enzyme recognition sites. For constructing the E1-deleted Ad, a two-plasmid system, that is, separate construction of the therapeutic gene and adenoviral backbone in two plasmids, was recently utilized.[23] However, when constructing CRAs, a modification of the E1 region is additionally necessary; currently, there is no standardized method to construct diverse types of m-CRAs in large numbers. Owing to this deficiency, many molecular biologists or gene therapy researchers, who are not CRA specialists, may not be able to efficiently construct CRAs, whereas they can feasibly construct E1-deleted Ad using commercially available kits. Detailed protocols, incorporating the careful consideration of available restriction enzyme sites, should be formulated each time a new CRA is constructed or any time a currently available CRA is modified. The procedures used currently may vary in the details of constructing different m-CRAs, and additional modifications of their own protocols in individual laboratories may be necessary depending on individual CRAs. Thus, even though it may be possible to construct an m-CRA, the present methods are not yet standardized and are deficient in their potential to be widely utilized by a large number of researchers.

In this respect, the notable feature of our system is that it allows the independent and unrestricted construction of individual elements of viral replication, therapeutic genes, and adenoviral backbones in three plasmids, and subsequently permits the accurate fusion of these plasmids within the same protocol into a single m-CRA plasmid without regular ligation procedures. This feature enables a normally trained molecular biologist to feasibly construct m-CRAs, and to construct and/or modify diverse m-CRAs in large numbers. To this end, we introduced *Cre/lox* recombination and I-*Ceu*I/PI-*Sce*I-based ligation for combining the three plasmids, and different types of antibiotic resistance genes and *ori* for specifically selecting only the correctly combined clones, into this system. In this context, the factors needed for this system to function at its maximum efficiency were the use of both an optimized concentration of tetracycline, and high-activity *Cre*. Due to the fact that there have been no reports of tetracycline selection together with the *Cre/lox* recombination in *E. coli*, and because we obtained a lower transformation efficiency with tetracycline than with kanamycin or ampicilin, we initially determined the optimal concentration of tetracycline for this system. Unexpectedly, the optimal concentration of tetracycline was 5 μg/ml in the LB plate, which is lower than that described in textbooks (12 μg/ml),[27] and the effective range was narrow (data not shown). Higher *Cre* activity is also essential, especially due to the use of tetracycline selection; the use of lower *Cre* activity did not result in the appearance of the correct clone. We established a feasible and inexpensive way to obtain aliquots containing highly active *Cre*. With these conditions, sufficient numbers of clones always appeared, and all of them contained the correct recombined plasmid. The distinct advantage of the present method is 100% accuracy of correct clones among all of the transformed clones in *E. coli*; this feature, together with the use of miniprep DNA throughout the procedure, allowed us to handle multiple diverse samples at one time, and we in fact simultaneously constructed diverse types of m-CRAs in this study. The remnant components of *tet*^{r}, *R6Kγ ori*, and a single *lox* sequence in m-CRAs, which are indispensable to achieve 100% accuracy of correct clones,

are not troublesome, at least for the experimental purpose, probably in general, described herein because neither *tet*^{r} lacking a proper mammalian promoter or poly A sequence, nor *R6Kγ ori* efficiently function in mammalian cells. In fact, we found that several m-CRAs, including the ones shown in Figure 3c in this study, function well with these components without any harmful effects.

An introduction of a marker gene into a CRA, such as *EGFP* gene used in the present study, which allows researchers to monitor the spread of a CRA *in vitro* and *in vivo*, is quite useful for carefully analyzing the virological features of CRA. It was recently shown that CRA expressing a therapeutic gene may enhance the cytotoxicity and the therapeutic potential in addition to the oncolytic activity of CRAs.[19] In this regard, an advantage of our system is the ability to subsequently insert a therapeutic or marker gene either into an m-CRA plasmid in *E. coli* or directly into m-CRA in *Cre*-expressing 293 cells. To maximize both protocols, diverse types of P1+3 and P2 may be initially prepared using the regular subcloning procedure, because combining different types of P1+3 and P2 at the later stage can be carried out simultaneously, as shown in the present study. The latter protocol, that is, direct transfection of P1+3 and P2 into *Cre*-expressing 293 cells, has the advantage of further eliminating one step in *E. coli*, leading to an increase in the rapidity of the procedure. *EGFP* or other fluorescent genes alongside the therapeutic gene in P2, which allows direct identification of the correct m-CRA plaque containing therapeutic genes under fluorescent microscopy, may maximize this benefit.

The unrestricted and independent construction of individual elements in the three-plasmid system should not only expedite the process of generating diverse m-CRAs but also make feasible the modification of individual elements in m-CRAs. Several combination patterns of different P1, P2, and P3 vectors allow the generation of diverse types of m-CRAs in large numbers, including those in which some elements were modified with diverse combinations. Lessons from previous gene therapy studies, that is, discrepancies between experimental data and actual clinical outcomes, suggest the necessity of the systematic and extensive examination of the biological and virological characteristics of diverse m-CRAs in practice. In this respect, the ability to efficiently generate large numbers of modified m-CRAs with diverse combinations of gene elements may be the most significant advantage of our system. Particularly, unrestricted selection of the adenoviral backbone may provide two potential advantages. First, any suitable adenoviral backbone, such as fiber-modified Ads to achieve tumor-specific infection, which may be determined by other types of extensive studies, can be directly used in the m-CRA studies; additional steps in constructing new m-CRAs that contain both characteristic elements may be omitted. Second, Ad can package 105% of its genome, and such DNA size limitation may potentially complicate or hamper the modification of pre-constructed m-CRAs. However, the present system allows the change of the P3 backbone plasmid to circumvent this problem; P3 with a longer deletion can be used if additional DNA should be inserted in P1 or P2 to modify pre-established m-CRA. Namely, the three-plasmid system in the present m-CRA construction may maximize the benefit of the *in vitro* ligation system.[23] For instance, up to 5.4, 5.9 or 8.7 kb of DNA elements can be introduced in P1 and P2 when pAdHM4, pAdHM10, or pAdHM12 is used as P3 vector, respectively, as described previously.[23]

In conclusion, the present study reports a novel method for efficiently constructing and/or modifying diverse m-CRAs; this system may be useful for the development of the ideal m-CRA for tumor therapy.

Materials and methods

Cell lines

The human hepatoma cell line, Hep-G2, was obtained from the Cell Resource Center for Biomedical Research at the Institute of Development, Aging and Cancer, Tohoku University (Sendai, Japan). Hep-G2 was cultured in Dulbecco's modified Eagle's medium supplemented with 100 U/ml penicillin, 100 μg/ml streptomycin, and 10% fetal bovine serum. The *Cre*-expressing 293 cell line was generated as described elsewhere.[28]

Plasmids

Plasmid P1 was constructed as follows. The E1A coding sequence and pA without the native E1A promoter were obtained by PCR from pXC1 (Microbix, Toronto, Canada) with the primers S-E1A/AS-E1A (Table 1). This E1A fragment was digested with *Sph*I and *Sal*I and inserted into *Sph*I/*Sal*I-digested pHM5.[23] The resulting plasmid was designated pΔPrE1A. The mt E1B coding sequence (1684–2285), which lacked the E1B55kD coding sequence, native E1B promoter, and pA, was obtained by PCR from pXC1 with the primers S-E1BΔ55kD/AS-E1BΔ55kD (Table 1) and inserted into pΔPrE1A by *Sal*I/*BamH*I sites, resulting in pΔPrE1A-ΔPrE1BΔ55kDΔpA plasmid. BGHpA obtained by PCR with the primers S-BGHpA/AS-BGHpA (Table 1) from pRc/CMV plasmid (Invitrogen, Carlsbad, CA, USA) was inserted into pΔPrE1A-ΔPrE1BΔ55kDΔpA by *BamH*I/*Eco*RI sites, resulting in pΔPrE1A-ΔPrE1BΔ55kD plasmid. The full length of E1B (1684–4073) was obtained by PCR from pXC1 with the primers S-E1B/AS-E1B (Table 1) and inserted into *Kpn*I/*Eco*RI-digested pΔPrE1A-ΔPrE1BΔ55kD, resulting in ΔPrE1A-ΔPrE1B plasmid. All sequences obtained by PCR were confirmed using an ABI Prism 310 genetic analyzer (Applied Biosystems, Foster City, CA, USA).

E1A sequence without a 24 bp sequence for pRb binding was obtained by site-directed mutagenesis using sequential PCR steps[27] with the primers AS-E1AΔ24/S-E1AΔ24 (Table 1). The obtained product was inserted into pΔPrE1A-ΔPrE1B or pΔPrE1A-ΔPrE1BΔ55kD plasmid by *Not*I/*Sal*I sites, resulting in pΔPrE1AΔ24-ΔPrE1B or pΔPrE1AΔ24-ΔPrE1BΔ55kD plasmid, respectively.

Plasmid P2 was constructed as follows. *kan*^{r} was removed from pUni/V5-HisC (Invitrogen) by *Bgl*II/*Sma*I digestion. A blunt-end fragment of *tet*^{r} obtained from pBR322 (Invitrogen) was inserted into the vector to yield pUni/V5-HisC-*tet*^{r}. The construction of plasmid P3 was performed as described previously.[23]

CEApr[29] and CMVpr were obtained by PCR from AxCEAprTK (Riken gene bank, Tsukuba, Japan) and pRc/CMV with the primer sets of S-CEApr/AS-CEApr and S-CMVpr/AS-CMVpr, respectively (Table 1). The fragment containing CEApr or CMVpr was excised by

Table 1 PCR primers

Primer	*Sequence*	*Annealing temperature (°C)*
S-E1A	5′-TCAGTCGCATGCGCGGCCGCTACGTAACGCGTTACCCGGTGAGTTCCTCAAGAGGC-3′	57
AS-E1A	5′-GGACGTCCTAGGGTCGACGCCCCATTTAACACGCCATGCAAG-3′	
S-E1BΔ55kD	5′-TCAGTCCCTAGGGTCGACCATATGGATATCCAATTGCGTGGGCTAATCTTGGTTACATCT-3′	57
AS-E1BΔ55kD	5′-GGACGTGGATCCGCGTCTCAGTTCTGGATACAGTTC-3′	
S-E1B	5′ATAAATGGAGCGAAGAAACC -3′	57
AS-E1B	5′-GGACGTGAATTCATAACTTCGTATAATGTATGCTATATGAGGTAATCTTGATCCAAATCCAAACAGAGTC-3′	
S-BGHpA	5′-TCAGTCGGATCCGCATGCATCTAGAGCTCGCTGATC-3′	57
AS-BGHpA	5′-GGACGTGAATTCATAACTTCGTATAATGTATGCTATATGAGGTAATTCAGAAGCCATAGAGCCCACCGCA-3′	
S-Δ24	5′-TTGTACCGGAGGTGATCGATCCACCCAGT-3′	57
AS-Δ24	5′-TCCTCGTCGTCACTGGGTGGATCGATCACC-3′	
S-CEApr	5′-TCAGTCGCGGCCGCATCATCCCACCTTCCCAGAG-3′	57
AS-CEApr	5′-GGACGTACGCGTCCATGGTCTCTGCTGTCTGC-3′	
S-CMVpr	5′-TCAGTCGTCGACCGTTGACATTGATTATTGAC-3′	57
AS-CMVpr	5′-GGACGTCAATTGGCTTGGGTCTCCCTATAGTG-3′	
S-E1A-1	5′-CCTGTGGCATGTTTGTCTAC-3′	57
AS-E1A-1	5′-CAACTGGTTTAATGGGGCAC-3′	
S-E1B-1	5′-AAGGAGGATTACAAGTGGGA-3′	57
AS-E1B-1	5′-AGTAGCAGGCGATTCTTGTG-3′	
S-EGFP	5′-CACAAGTTCAGCGTGTCC-3′	59
AS-EGFP	5′-CTTGATGCCGTTCTTCTG-3′	
S-Fiber	5′-GTTCCTGTCCATCCGCACCCACTATCTTCATGTTG-3′	59
AS-Fiber	5′-AGTGGCAGTAGTTAGAGGGGGTGAGGCAGTGATAG-3′	
S-pHM5	5′-AACGGTCCTAAGGTAGCGAA-3′	59

*Not*I/*Mlu*I or *Sal*I/*Mfe*I, respectively, and ligated into similarly digested pΔPrE1A-ΔPrE1BΔ55kD or pΔPrE1AΔ24-ΔPrE1BΔ55kD, resulting in pCEApr-E1A-CMVpr-E1BΔ55kD or pCEApr-E1AΔ24-CMVpr-E1BΔ55kD. Human osteocalcin promoter (OCpr, −834 to +34)[30] and Surv.pr (−173 to −19)[31] were obtained by PCR from genomic DNA (details should be described elsewhere). E2Fpr (−218 to +51)[32] and TERTpr (−181 to +78)[33] were kindly provided by H Fine (National Cancer Institute, Bethesda, MD, USA) and S Kyo (Kanazawa University, Kanazawa, Japan), respectively. P1 plasmids pCEApr-E1A-E2Fpr-E1BΔ55kD, pCEApr-E1AΔ24-E2Fpr-E1BΔ55kD, pE2Fpr-E1A-CMVpr-E1BΔ55kD, pE2Fpr-E1AΔ24-CMVpr-E1BΔ55kD, pOCpr-E1A-CMVpr-E1BΔ55kD, pOCpr-E1AΔ24-CMVpr-E1BΔ55kD, pTERTpr-E1A-CMVpr-E1BΔ55kD, pTERTpr-E1AΔ24-CMVpr-E1BΔ55kD, pTERTpr-E1A-E2Fpr-E1BΔ55kD, and pTERTpr-E1AΔ24-E2Fpr-E1BΔ55kD were constructed in the same manner as described above. pUni/V5-HisC-*tet*^{r} was digested with *Xho*I and blunted, and the blunt-end fragment of CMVpr, which was excised from pCEApr-E1A-CMVpr-E1BΔ55kD, was inserted to yield pUni/CMVpr. The EGFP coding sequence from pEGFP-C1 (Clontech, Palo Alto, CA, USA) was inserted into pUni/CMVpr to obtain pUni/CMVpr-EGFP. In the same manner, Surv.pr was inserted into pUni/V5-HisC-*tet*^{r}, resulting in pUni/Surv.pr. pUni/CMVpr-p53, pUni/CMVpr-tk, pUni/Surv.pr-p53, and pUni/Surv.pr-tk were constructed by insertion of p53 and HSV-tk fragment excised from pCMV-p53 (Clontech) and pAd.RSV-tk (kindly provided by Z Sheng Guo, University of Pittsburgh Cancer Institute, Pittsburgh, PA, USA) into pUni/CMVpr or pUni/Surv.pr.

PCR

The primer sets used in this study are listed in Table 1. The PCR conditions that were used for the m-CRA construction are described earlier. For verification of the correct m-CRAs, PCR of genomic DNA, which was extracted from viral plaques with proteinase K digestion phenol/chloroform purification and ethanol precipitation, was performed with primer sets, as shown in Table 1. The amplified DNA was analyzed by electrophoresis on 1% agarose gel.

Preparation of Ads

All Ads were generated and amplified in 293 cells, and purified in CsCl gradients, as described previously.[5,23] The titer of the Ads (plaque-forming unit/ml) was measured by a plaque assay on 293 cells.

Acknowledgements

This study was supported in part by a grant for Cooperation of Innovative Technology and Advanced Research in Evolutional Area (CITY AREA) and a Grant-in-Aid for Scientific Research on Priority Areas (C) from the Ministry of Education, Culture, Sports, Science and Technology, Japan, a grant from the Uehara Memorial Foundation and Health and Labour Sciences Research Grants for Third Term Comprehensive Control Research for Cancer from the Ministry of Health, Labour and Welfare, Japan. We thank Izumu Saito, Jun-ichi Miyazaki, Howard Fine, Satoru Kyo, Z Sheng Guo, and Mark A Kay for providing materials and David Cochran for editing the manuscript.

References

1 Terazaki Y *et al*. An optimal therapeutic expression level is crucial for suicide gene therapy for hepatic metastatic cancer in mice. *Hepatology* 2003; **37**: 155–163.

2 Fukunaga M *et al.* Adenoviral herpes simplex virus thymidine kinase gene therapy in an orthotopic lung cancer model. *Ann Thorac Surg* 2002; **73**: 1740–1746.
3 Caruso M *et al.* Adenovirus-mediated interleukin-12 gene therapy for metastatic colon carcinoma. *Proc Natl Acad Sci USA* 1996; **93**: 11302–11306.
4 Nagano S *et al.* Gene therapy eradicating distant disseminated micro-metastases by optimal cytokine expression in the primary lesion only: novel concepts for successful cytokine gene therapy. *Int J Oncol* 2004; **24**: 549–558.
5 Chen SH *et al.* Combination gene therapy for liver metastasis of colon carcinoma *in vivo*. *Proc Natl Acad Sci USA* 1995; **92**: 2577–2581.
6 Kruyt FA, Curiel DT. Toward a new generation of conditionally replicating adenoviruses: pairing tumor selectivity with maximal oncolysis. *Hum Gene Ther* 2002; **13**: 485–495.
7 Hallden G, Thorne SH, Yang J, Kirn DH. Replication-selective oncolytic adenoviruses. *Methods Mol Med* 2004; **90**: 71–90.
8 Curiel DT. The development of conditionally replicative adenoviruses for cancer therapy. *Clin Cancer Res* 2000; **6**: 3395–3399.
9 Rodriguez R *et al.* Prostate attenuated replication competent adenovirus (ARCA) CN706: a selective cytotoxic for prostate-specific antigen-positive prostate cancer cells. *Cancer Res* 1997; **57**: 2559–2563.
10 Hallenbeck PL *et al.* A novel tumor-specific replication-restricted adenoviral vector for gene therapy of hepatocellular carcinoma. *Hum Gene Ther* 1999; **10**: 1721–1733.
11 Adachi Y *et al.* A midkine promoter-based conditionally replicative adenovirus for treatment of pediatric solid tumors and bone marrow tumor purging. *Cancer Res* 2001; **61**: 7882–7888.
12 Nettelbeck DM *et al.* Novel oncolytic adenoviruses targeted to melanoma: specific viral replication and cytolysis by expression of E1A mutants from the tyrosinase enhancer/promoter. *Cancer Res* 2002; **62**: 4663–4670.
13 Bischoff JR *et al.* An adenovirus mutant that replicates selectively in p53-deficient human tumor cells. *Science* 1996; **274**: 373–376.
14 Fueyo J *et al.* A mutant oncolytic adenovirus targeting the Rb pathway produces anti-glioma effect *in vivo*. *Oncogene* 2000; **19**: 2–12.
15 Heise C *et al.* An adenovirus E1A mutant that demonstrates potent and selective systemic anti-tumoral efficacy. *Nat Med* 2000; **6**: 1134–1139.
16 Shenk T. Adenoviridae: the viruses and their replication. In: Fields BN, Knipe DM, Howly PM (ed). *Fields Virology*. Lippincott-Raven: Philadelphia, 1996, pp 2111–2147.
17 Harada JN, Berk AJ. p53-Independent and -dependent requirements for E1B-55 K in adenovirus type 5 replication. *J Virol* 1999; **73**: 5333–5344.
18 Rothmann T *et al.* Replication of ONYX-015, a potential anticancer adenovirus, is independent of p53 status in tumor cells. *J Virol* 1998; **72**: 9470–9478.
19 Geoerger B *et al.* Oncolytic activity of p53-expressing conditionally replicative adenovirus Ad{Delta}24-p53 against human malignant glioma. *Cancer Res* 2004; **64**: 5753–5759.
20 Gomez-Manzano C *et al.* A novel E1A-E1B mutant adenovirus induces glioma regression *in vivo*. *Oncogene* 2004; **23**: 1821–1828.
21 Yu DC, Sakamoto GT, Henderson DR. Identification of the transcriptional regulatory sequences of human kallikrein 2 and their use in the construction of calydon virus 764, an attenuated replication competent adenovirus for prostate cancer therapy. *Cancer Res* 1999; **59**: 1498–1504.
22 Johnson L *et al.* Selectively replicating adenoviruses targeting deregulated E2F activity are potent, systemic antitumor agents. *Cancer Cell* 2002; **1**: 325–337.
23 Mizuguchi H, Kay MA. Efficient construction of a recombinant adenovirus vector by an improved *in vitro* ligation method. *Hum Gene Ther* 1998; **9**: 2577–2583.
24 Miyake S *et al.* Efficient generation of recombinant adenoviruses using adenovirus DNA-terminal protein complex and a cosmid bearing the full-length virus genome. *Proc Natl Acad Sci USA* 1996; **93**: 1320–1324.
25 Chartier C *et al.* Efficient generation of recombinant adenovirus vectors by homologous recombination in *Escherichia coli*. *J Virol* 1996; **70**: 4805–4810.
26 Metcalf WW, Jiang W, Wanner BL. Use of the rep technique for allele replacement to construct new *Escherichia coli* hosts for maintenance of R6 K gamma origin plasmids at different copy numbers. *Gene* 1994; **138**: 1–7.
27 Ausubel FM (ed). *Current Protocols in Molecular Biology*. John Wiley & Sons: New York, 1999.
28 Chen L, Anton M, Graham FL. Production and characterization of human 293 cell lines expressing the site-specific recombinase Cre. *Somat Cell Mol Genet* 1996; **22**: 477–488.
29 Osaki T *et al.* Gene therapy for carcinoembryonic antigen-producing human lung cancer cells by cell type-specific expression of herpes simplex virus thymidine kinase gene. *Cancer Res* 1994; **54**: 5258–5261.
30 Yeung F *et al.* Regulation of human osteocalcin promoter in hormone-independent human prostate cancer cells. *J Biol Chem* 2002; **277**: 2468–2476.
31 Li F, Altieri DC. The cancer antiapoptosis mouse survivin gene: characterization of locus and transcriptional requirements of basal and cell cycle-dependent expression. *Cancer Res* 1999; **59**: 3143–3151.
32 Parr MJ *et al.* Tumor-selective transgene expression *in vivo* mediated by an E2F-responsive adenoviral vector. *Nat Med* 1997; **3**: 1145–1149.
33 Takakura M *et al.* Cloning of human telomerase catalytic subunit (hTERT) gene promoter and identification of proximal core promoter sequences essential for transcriptional activation in immortalized and cancer cells. *Cancer Res* 1999; **59**: 551–557.

Supplementary Information accompanies the paper on Gene Therapy website (http://www.nature.com/gt)

Adenoviral gene transduction of hepatocyte growth factor elicits inhibitory effects for hepatoma

KENTARO YUGE[1,3], TOMOYUKI TAKAHASHI[1,4,7], SATOSHI NAGANO[7,8], YASUHIRO TERAZAKI[5], YOSHITERU MUROFUSHI[1,7], HIROAKI USHIKOSHI[1,2], TAKAO KAWAI[1,2], NGIN CIN KHAI[1,2], TOSHIKAZU NAKAMURA[9], HISAYOSHI FUJIWARA[2] and KEN-ICHIRO KOSAI[1,6,7]

[1]Department of Gene Therapy and Regenerative Medicine, Gifu University School of Medicine; [2]Department of Cardiology, Respiratory and Nephrology, Regeneration & Advanced Medical Science, Graduate School of Medicine, Gifu University, 1-1 Yanagido, Gifu 501-1194; [3]First Department of Internal Medicine, [4]Department of Advanced Therapeutics and Regenerative Medicine, Departments of [5]Surgery and [6]Pediatrics and Child Health, Kurume University School of Medicine, and [7]Division of Gene Therapy and Regenerative Medicine, Cognitive and Molecular Research Institute of Brain Diseases, Kurume University, 67 Asahi-machi, Kurume 830-0011; [8]Department of Orthopaedics, Faculty of Medicine, Kagoshima University, 8-35-1 Sakuragaoka, Kagoshima 890-8520; [9]Division of Molecular Regenerative Medicine, Course of Advanced Medicine, Osaka University Graduate School of Medicine, 2-2 Yamadaoka, Suita 565-0871, Japan

Received November 29, 2004; Accepted February 3, 2005

Abstract. Hepatocyte growth factor (HGF) gene therapy may have potential for treating chronic hepatitis (CH) and liver cirrhosis (LC). However, the lack of an HGF gene therapy study on hepatomas that are often associated with CH or LC, together with the stimulatory effects of HGF on many types of cancer, may hamper its application. This study explored the effects of adenoviral HGF gene transduction and their mechanisms on two types of hepatoma cells (hepatoblastoma and hepatocellular carcinoma) in *in vitro* experiments. Both types of hepatomas were revealed to have higher adenoviral gene transduction efficiencies and more efficient expressions of the HGF transgene, which successfully activated the HGF receptor/c-Met in an autocrine fashion, than those of other types of cancer. Notably, not only HGF, but also adenoviral infection, inhibited DNA synthesis, whereas only HGF but not adenoviral infection exerted a potent apoptotic effect. Moreover, adenoviral HGF gene transduction additively exerted inhibitory effects on cisplatin-treated hepatomas. In conclusion, inhibitory and apoptotic effects of adenoviral HGF gene transduction in hepatomas in contrast to potent mitogenic and antiapoptotic effects of HGF for hepatocytes are not only of biological interest, but also pose clinical benefits for adenoviral HGF gene therapy for CH and LC.

Correspondence to: Dr Ken-Ichiro Kosai, Division of Gene Therapy and Regenerative Medicine, Cognitive and Molecular Research Institute of Brain Diseases, Kurume University, 67 Asahi-machi, Kurume 830-0011, Japan
E-mail: kosai@med.kurume-u.ac.jp

Abbreviations: Ad, adenoviral vector; AGTE, adenoviral gene transduction efficiency; MOI, multiplicity of infection; RSV, Rous sarcoma virus long terminal repeat; X-gal, o-nitrophenyl-ß-D-galactophyranoside; ELISA, enzyme-linked immunosorbent assay

Key words: adenoviral vector, hepatocyte growth factor, hepatoma, apoptosis, DNA synthesis, cisplatin

Introduction

Hepatocyte growth factor (HGF), originally identified (1-4) and cloned (5,6) as a potent mitogen for hepatocytes, is a multifunctional cytokine that exhibits mitogenic, motogenic, morphologic, angiogeneic, antiapoptotic and organotrophic effects on a variety of tissues (7). We recently showed that HGF exerts a potent antiapoptotic effect on hepatocytes and antifibrotic effects, and can be used to treat acute hepatitis, including fulminant hepatic failure (8,9), and chronic hepatitis (CH) and liver cirrhosis (LC) in animals (10-12). Thus, these beneficial effects, together with the inducible effect for liver regeneration (13), suggest that HGF gene therapy may be a promising treatment for CH and LC.

However, certain types of growth factors may play important roles in the carcinogenesis, tumor growth, and angiogenesis of cancer. Accumulating data suggest that HGF may enhance the growth and metastases of a majority of cancers, probably due not only to direct stimulation of cancer cell growth, but to the enhancement of angiogenesis (14,15). In fact, the HGF antagonist has been shown to inhibit cancer cell growth, metastasis, and angiogenesis of some cancers in animals (16,17). In contrast, other studies suggested that HGF might exert an inhibitory effect on certain types of cancers (18-23) although their overall features and mechanisms remain obscure.

In particular, the roles and effects of HGF on hepatomas remain largely controversial. In transgenic mouse (Tg) studies,

two distinct types of HGF Tg, in which HGF was over-expressed under the transcriptional control of either the hepatocyte-specific albumin promoter (Alb-HGF-Tg) (24) or the ubiquitously active mouse metallothionein gene promoter (MT-HGF-Tg) (25,26), demonstrated completely opposite results concerning hepatocarcinogenesis. Alb-HGF-Tg never formed a hepatocellular carcinoma (HCC), and furthermore, analyses using two kinds of double Tg; Alb-HGF/MT-TGF-α Tg (27) and Alb-HGF/Alb-*c-myc*-Tg (28), showed that the overexpression of HGF in hepatocytes inhibited both TGF-α and c-myc-induced hepatocarcinogenesis. In contrast, MT-HGF-Tg formed cancers in several organs, including HCC in the liver (25,26). Thus, rather than elucidating this issue, these Tg studies have led to confusion, probably due to the artificial factors in the studies. On the other hand, *in vitro* studies have recently shown that recombinant HGF has an inhibitory effect on the human hepatoblastoma cell line, HepG2 (29), but no study has as yet explored the effects of HGF on human hepatocellular carcinoma (HCC). More importantly, there has not only been no direct studies of HGF gene therapy for hepatoma, but also no biological studies of adenoviral HGF gene transduction in hepatomas, including no investigation of the effects of adenoviral infection itself or the effects of exogenous HGF gene expression in an artificial autocrine fashion.

HCC, which is the major type of hepatoma found in adult patients, is usually associated with CH or LC. Alternatively, CH and LC have a high risk of hepatocarcinogenesis (30-32), and some patients with CH and/or LC may potentially have latent HCC at an undetectably small size. Thus, although HGF gene therapy may have potential for treating CH and LC, its clinical application may be prohibited due to the uncertain effects of HGF gene therapy for hepatomas. In this regard, the present study biologically explored the effect of adenoviral HGF gene transduction in hepatoma cells and its mechanism.

Materials and methods

Human cell lines. The human cell lines Hep3B (HCC), HepG2 (hepatoblastoma), HeLa (cervical carcinoma), MKN-28 (gastric carcinoma), colo-205 (colon carcinoma), HOS-NP (osteosarcoma), A549 (lung carcinoma) and 293, were cultured in 5% CO_2 at 37˚C in Dulbecco's modified Eagle's medium supplemented with penicillin/streptomycin and 10% fetal calf serum.

Recombinant adenoviral vectors (Ads) and adenoviral gene transduction efficiencies (AGTEs). Replication-defective Ads, Ad.RSV-HGF and Ad.RSV-LacZ, which encode the human HGF and ß-galactosidase gene, respectively, downstream of the transcriptional control of the Rous sarcoma virus long terminal repeat (RSV) promoter were constructed, prepared, and titered as described previously (33-35). AGTEs were assessed by 5-bromo-4-chloro-3-indolyl-ß-D-galacto-pyranoside (X-gal) staining after Ad.RSV-LacZ infection, as described previously (36-38).

HGF enzyme-linked immunosorbent assay (ELISA). HeLa, Hep3B and HepG2 cells at 1000, 1000 and 2000 cells/well in 96-well plates, respectively, were infected with Ad.RSV-HGF, and the supernatant was collected 48 or 96 h later. The human HGF levels in the supernatant were measured by ELISA according to the manufacturer's protocol (R&D Systems, Inc., Minneapolis, MN).

C-Met phosphorylation. C-Met phosphorylation in the cells was detected by the immunoprecipitation method (39). Briefly, the cells were lysed in 500 µl RIPA buffer (1% Triton X, 150 mM NaCl, 50 mM Tris-HCl pH 7.6, 10% glycerol, 1 mM Vanadate, 1 mM phenylmethylsulfonyl fluoride) with protease inhibitors after incubation with the serum-free media for 24 h and subsequently with new serum-free media containing recombinant HGF (R&D Systems) or the supernatant from Ad.RSV-HGF-infected HepG2 cells for 10 min. After centrifugation, the supernatant was incubated with 0.5 ng/ml anti-c-Met monoclonal antibody (C-12, Santa Cruz Biotechnology, Inc., Santa Cruz, CA) for 4 h, and sequentially incubated with 10 µl Protein G Sepharose beads for 3 h. The proteins bound to beads were dissolved in sample buffer and subjected to sodium dodecyl sulfate-polyacrylamide gel electrophoresis (SDS-PAGE). Phosphorylated c-Met was immunoblotted with anti-phosphotyrosine antibody (PY20, Transduction Laboratories, Lexington, KY).

WST-8 cell viability assay. The cells were infected with each Ad in the same manner as in the HGF ELISA experiment. Cell viability was determined by WST-8 assay (Dojindo Laboratories Co., Mashiki, Japan) at 2, 4, 6 or 8 days after Ad infection according to the manufacturer's protocol (36,37).

To explore the effect of HGF in cisplatin (cis-Diammine-dichloroplatinum (II))-treated hepatoma cells, cisplatin was added to the media in the HepG2 and HeLa cells (125 µg/ml) and in the Hep3B cells (250 µg/ml) at 24 h after Ad-infection.

Bromo-2'-deoxyuridine (BrdU) uptake assay. The cells were infected with each Ad in the same manner as in the HGF ELISA experiments. Four days later, the cells were incubated with 10 µM of BrdU for 4 h and harvested. The percentage of cells that had BrdU uptake was measured by ELISA according to the manufacturer's protocol (BrdU Labeling and Detection Kit III, Roche Diagnostics GmbH, Mannheim, Germany).

Terminal deoxynucleotidyl transferase-mediated deoxyuridine triphosphate biotin nick-end labelling (TUNEL) assay. Hep3B or HeLa ($1x10^5$) cells, or HepG2 ($2x10^5$) cells were infected with each Ad, and apoptotic cells were detected at 2, 4, 6 or 8 days later using an ApopTag Peroxidase *in situ* Apoptosis Detection Kit (Intergen Company, New York, USA) according to the manufacturer's protocols.

Detection of active form of caspase-3. The cells were lysed in hypotonic buffer (25 mM HEPES pH 7.5, 5 mmol/l $MgCl_2$, 1 mmol/l EDTA, 1 mmol/l phenylmethylsulfonyl fluoride) with protease inhibitors at 2, 3 or 4 days after adenoviral infection at the multiplicity of infection (MOI) of 10. Protein (30 µg) was subjected to SDS-PAGE, and Western blotting was performed using anti-caspase-3 antibody (BD Pharmingen, San Diego, CA), peroxidase-conjugated anti-rabbit IgG and

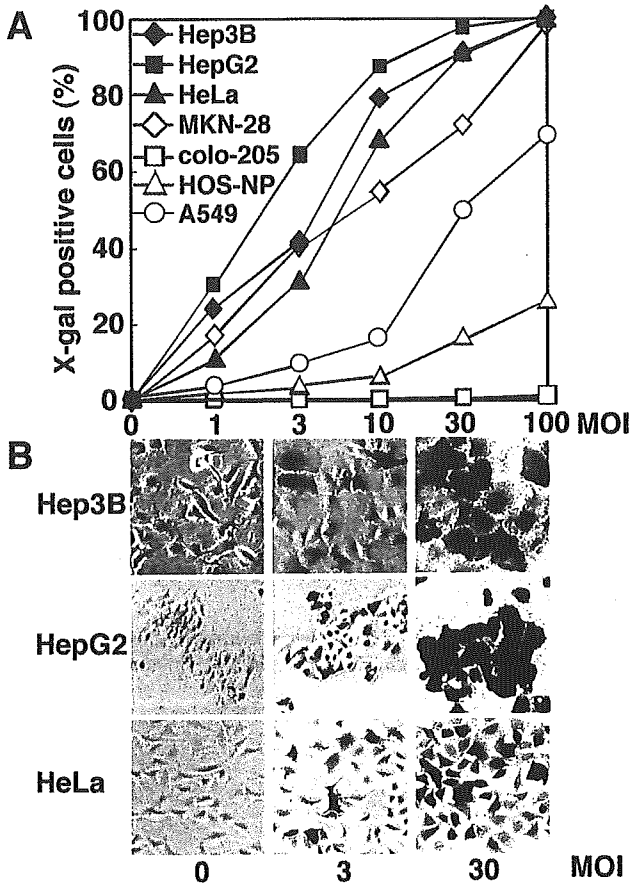

Figure 1. AGTEs. Cells were infected with Ad.RSV-LacZ at indicated MOIs and stained with X-gal. (A), The AGTEs in Hep3B and HepG2 were as high as those in HeLa cells, and higher than those in other types of cells. (B), The representative pictures of X-gal-stained cells.

SuperSignal® West Pico Chemiluminescent Substrate (Pierce Chemical Co., Rockford, IL).

Statistical analysis. All results are expressed as mean ± standard deviation. Statistical comparison were made using Student's t-test.

Results

High AGTE and HGF expression in hepatoma cells. The AGTEs in the Hep3B and HepG2 cells were as high as those in the HeLa cells, and higher than those in other types of human carcinoma cell lines at each MOI (Fig. 1). Because of this, the HeLa cells were chosen as a control for subsequent experiments.

The exogenous human HGF levels in the supernatant were much higher at 48 h than at 96 h after the Ad.RSV-HGF infection in the Hep3B, HepG2 and HeLa cells (Table I). The HGF levels largely differed among these 3 cell lines, and the levels in the HepG2 and Hep3B cells were remarkably higher than those in the HeLa cells at each point. In addition, the HGF levels in the supernatant from the Ad.RSV-HGF-infected MKN-28 cells were much lower than those of the HeLa cells (data not shown). Thus, hepatoma may be a good target for adenoviral HGF gene therapy in terms of the efficient secretion of exogenous HGF in the autocrine mode as well as a high AGTE.

Table I. HGF levels after adenoviral HGF gene transduction.

		HGF levels (ng/ml)	
Cell lines	MOIs	48 h	96 h
Hep3B	0	0.0	0.0
	3	<0.1	0.1
	10	0.1	6.0
	30	1.1	21.7
HepG2	0	0.0	0.0
	3	<0.1	2.1
	10	0.4	83.4
	30	5.9	>4125.0
HeLa	0	0.0	0.0
	3	<0.1	<0.1
	10	<0.1	0.1
	30	0.1	2.7

The supernatant was collected 48 or 96 h after infection with Ad.RSV-HGF at indicated MOIs. The human HGF levels in the supernatant was measured by ELISA.

Exogenous HGF in the autocrine fashion activates HGF receptor/c-Met. Immunoprecipitation and Western blot analysis showed that the Hep3B, HepG2, and HeLa cells were all abundant in the c-Met, which was similarly phosphorylated (i.e., activated) in an HGF dose-dependent manner (Fig. 2A).

HGF natively acts on target cells in a paracrine fashion in the body. Namely, a single chain prepro HGF is secreted from mesenchymal cells and then converted by a specific protease to biologically active mature HGF, which binds to c-Met and confers a biological function in hepatocytes (7). To explore whether transduced HGF in hepatoma cells may function in an artificial autocrine fashion, we initially tried to directly detect c-Met phosphorylation in the Ad.RSV-HGF-infected HepG2 and Hep3B cells. However, several attempts did not result in successful detection because it was difficult to detect short term c-Met phosphorylation under biologically complex circumstances in which persistent HGF expression might lead to repeated cycles of activation, downregulation and the revival of c-Met. Therefore, we indirectly explored the above issue as follows. The supernatant was collected from Ad.RSV-HGF-infected HepG2 cells, and the HGF concentration in it was measured. Subsequently, supernatant or recombinant HGF at the same concentration was added to intact HepG2 (Fig. 2B) or Hep3B cells (data not shown), and the c-Met phosphorylation was explored. As a result, c-Met activation was found to occur in both types of hepatomas in a dose-dependent manner similar to the cases of additions of recombinant HGF, indicating that exogenous HGF protein from the transgene might be efficiently converted to the active form by proteases natively present in the serum, and finally verifying that exogenous HGF correctly activated c-Met.

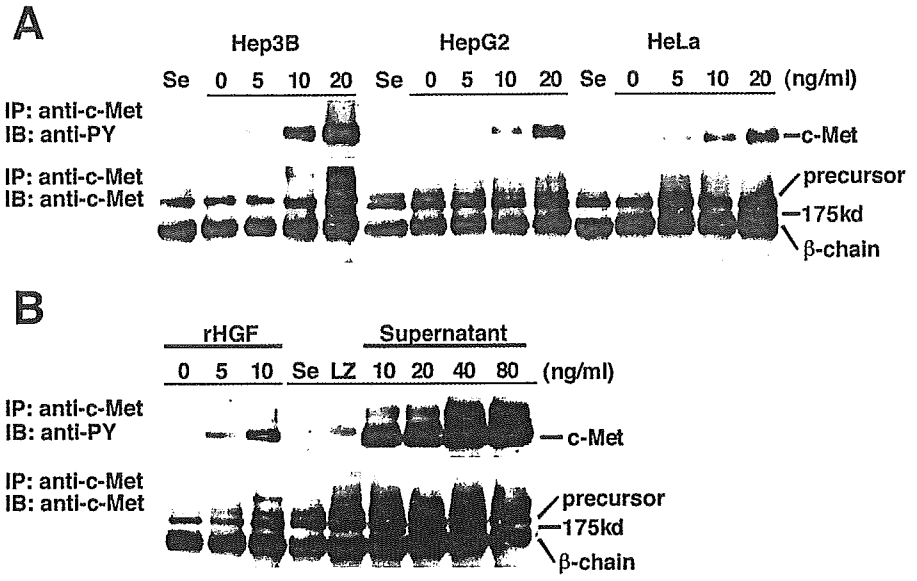

Figure 2. HGF receptor/c-Met and its activation. (A), Hep3B, HepG2 and HeLa cells were abundant in the c-Met, which was similarly phosphorylated in a HGF dose-dependent manner. (B), The c-Met on intact HepG2 cells was similarly phosphorylated by additions of the supernatant from Ad.RSV-HGF-infected HepG2 cells. IP, immunoprecipitation. IB, immunoblot. rHGF, recombinant HGF.

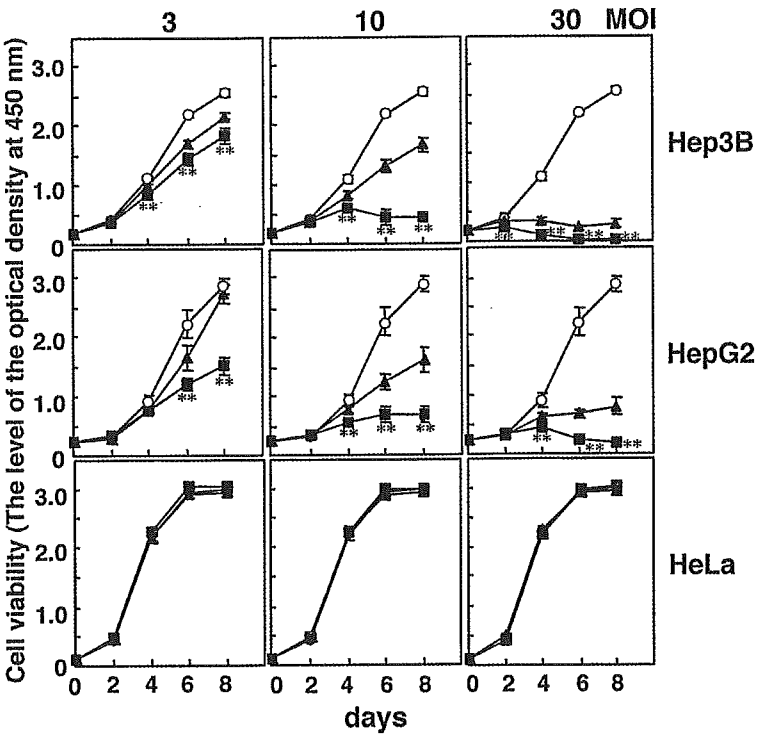

Figure 3. Inhibitory effects of adenoviral HGF gene transduction. Cell viability was determined by WST-8 assay 2, 4, 6 or 8 days after infection with each Ad at indicated MOIs. Although Ad.RSV-LacZ infection as well as Ad.RSV-HGF infection revealed some inhibitory effects for the HepG2 and Hep3B cells, but not for the HeLa cells, the degree of this inhibitory effect was more prominent in the Ad.RSV-HGF-infected cells (square) than the Ad.RSV-LacZ-infected ones (triangle). *P<0.05; **P<0.01 (Ad.RSV-HGF versus Ad.RSV-LacZ groups on each day at each MOI). No treatment control, circle. N=8, each point in each group.

Ad.RSV-HGF infection exerts inhibitory effects for hepatoma cells. The WST-8 assay showed that the number of viable Hep3B and HepG2 cells was significantly smaller in the Ad.RSV-HGF-infected cells than in the Ad.RSV-LacZ-infected cells at each MOI (Fig. 3). In addition, the infection of Ad.RSV-LacZ revealed some inhibitory effects for the HepG2 and Hep3B cells in an Ad dose-dependent manner, but not for the control HeLa cells, although the degree of this inhibitory effect was milder than that by Ad.RSV-HGF. In contrast, there was no difference in the number of viable HeLa cells among the Ad.RSV-HGF-infected, Ad.RSV-LacZ-infected cells, or no Ad-infected cells at any points. Thus,

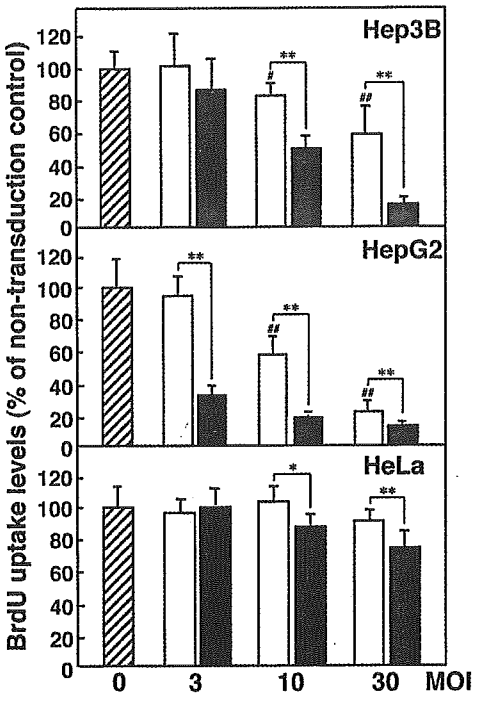

Figure 4. Inhibition of DNA synthesis. BrdU uptake assay was done 4 days after each Ad infection at indicated MOIs. Although the BrdU uptake levels were reduced by Ad.RSV-LacZ infection as well as Ad.RSV-HGF infection in HepG2 and Hep3B cells, the degree of this reduction was more prominent in the Ad.RSV-HGF-infected cells than the Ad.RSV-LacZ-infected ones. The BrdU uptake levels in HeLa cells were mildly reduced by Ad.RSV-HGF infection. *P<0.05; **P<0.01 (Ad.RSV-HGF groups versus Ad.RSV-LacZ groups at each MOI). #P<0.05; ##P<0.01 (Ad.RSV-LacZ versus non-transduced control). N=8, each point in each group.

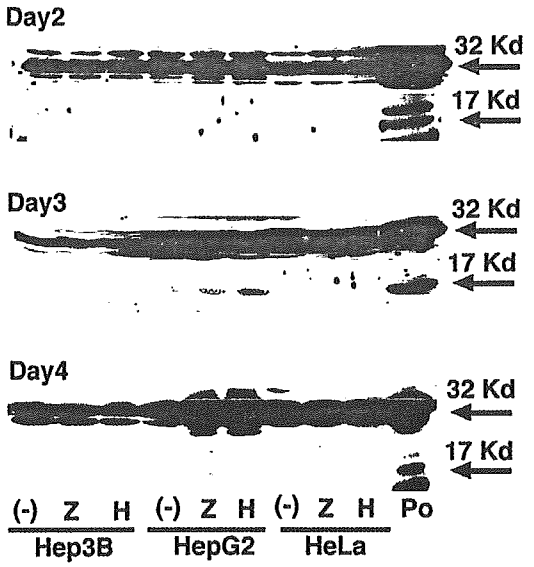

Figure 5. Caspase-3 activation. Pro-caspase-3 (32 kDa) and active caspase-3 (17 kDa) were detected by Western blotting of cells 2, 3, 4 days after no Ad (-), Ad.RSV-LacZ (Z) or Ad.RSV-HGF (H) infection at MOI of 10. Positive control (Po); cisplatin-treated HepG2 cells. More prominent activation of caspase-3 was seen in HepG2 cells 3 days after Ad.RSV-HGF infection than after Ad.RSV-LacZ or no Ad infection.

both types of hepatomas were remarkably sensitive not only to HGF, but also to the adenoviral infection itself, both of which independently and additively exerted inhibitory effects.

Ad.RSV-HGF infection inhibits DNA syntheses of hepatoma cells. There are two possible causes of inhibitory effects; one is the inhibition of cell growth, and the other is the induction of cell death. To assess the former, DNA replication was analyzed by the BrdU uptake assay (Fig. 4). The BrdU uptake levels in the Hep3B and HepG2 cells were both significantly reduced by not only Ad.RSV-HGF, but also by Ad.RSV-LacZ infection in an Ad dose-dependent manner. Statistical differences between the Ad.RSV-HGF and Ad.RSV-LacZ groups at each MOI further indicated that HGF itself inhibited cell growth in both types of hepatomas. The BrdU uptake levels in the HeLa cells were reduced only by Ad.RSV-HGF infection at a high MOI, but not by the adenovirus infection itself. Thus, not only HGF, but also the adenoviral infection itself, independently and additively inhibits cell growth in both types of hepatomas.

HGF but not adenoviral infection exerts apoptotic effect for hepatoma cells. To investigate the apoptotic effect of HGF on hepatomas, the activation of caspase-3, which leads to the activation of important apoptosis-related proteins such as caspase-activated DNase (40) and Acinus (41), was investigated by Western blotting (Fig. 5). Ad.RSV-HGF infection in the HepG2 cells led to a more prominent appearance of the active form of caspase-3 (17 kDa) than that of Ad.RSV-LacZ or no Ad infection. In contrast, a significant activation of caspase-3 was not detected in the Hep3B or HeLa cells after Ad.RSV-HGF, Ad.RSV-LacZ or no Ad infection, despite several trials. In addition, the activation of caspase-3 was not detected in any samples using the CPP32/Caspase-3 Colorimetric Protease Assay Kit (data not shown). Thus, despite substantial technical difficulty with this experimental system, including the issue of abundant pro-caspase-3 in comparison to a limited amount of active caspase-3, the detection of a more prominent band of active caspase-3 in the Ad.RSV-HGF-infected HepG2 cells suggests that exogenous HGF in the autocrine fashion may activate apoptotic signals in hepatoma cells.

We next performed TUNEL assays, which provided clearer and more definitive results (Fig. 6). TUNEL-positive Hep3B and HepG2 cells were significantly increased after the Ad.RSV-HGF infection, in contrast to no increase after the Ad.RSV-LacZ infection. On the other hand, TUNEL-positive HeLa cells were not seen after the Ad.RSV-HGF or Ad.RSV-LacZ infection. These findings indicate that HGF in an autocrine fashion may directly exert a potent apoptotic effect for both types of hepatomas; however, adenoviral infection itself does not induce apoptosis, in contrast to its inhibitory effect on cell growth.

Ad.RSV-HGF infection additively exerts inhibitory effect for cisplatin-treated hepatoma cells. To explore whether adenoviral HGF gene therapy is potentially applicable to hepatoma patients who undergo conventional carcinostatic treatments, we investigated the effect of Ad.RSV-HGF infection on cisplatin-treated hepatoma cells (Fig. 7). We chose cisplatin because cisplatin is one of the representative

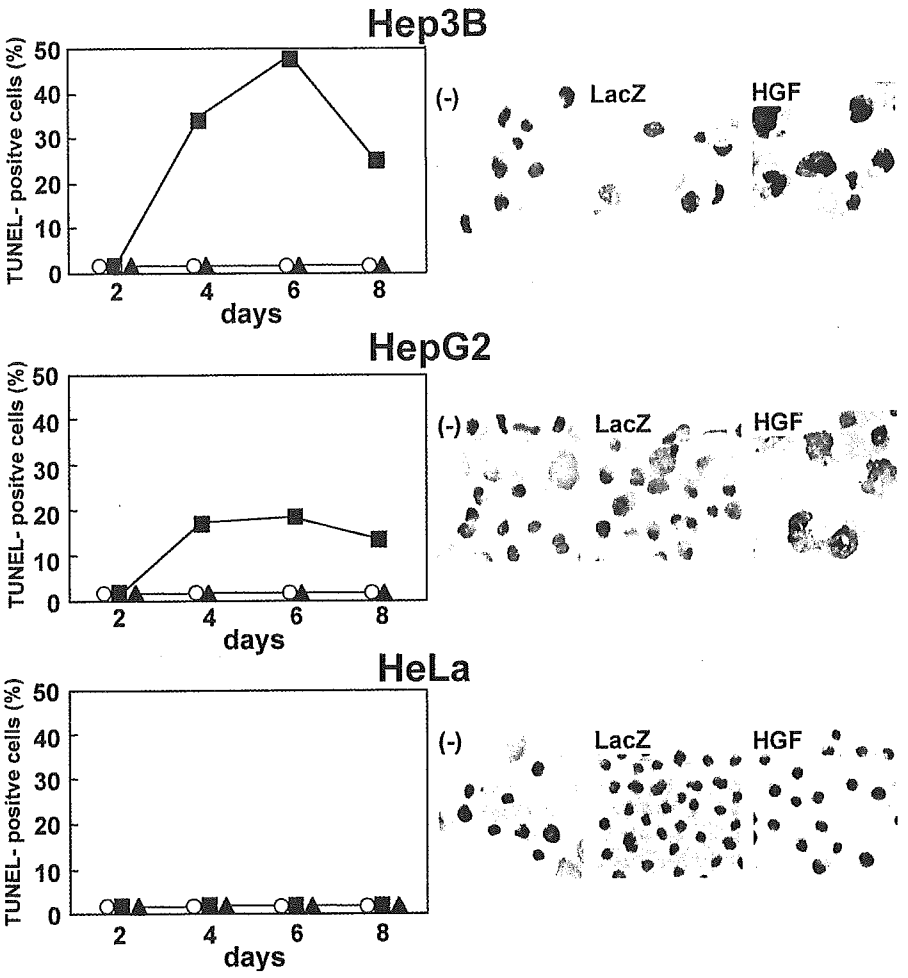

Figure 6. TUNEL assay. TUNEL-positive cells were significantly increased after Ad.RSV-HGF infection in Hep3B and HepG2 cells, but not in HeLa cells. In contrast, TULEL-positive cells were not seen after Ad.RSV-LacZ infection or control (no Ad infection). The circle, triangle and square symbols indicate no Ad-, Ad.RSV-LacZ- or Ad.RSV-HGF-treated groups, respectively. The representative pictures of TUNEL-positive cells 6 days after each Ad infection are shown in the right panel.

carcinostatics for hepatoma patients, especially in the case of transcatheter arterial embolization (TAE) therapy (42,43). WST-8 analysis showed that the Ad.RSV-HGF infection exerted additional inhibitory effects on both Hep3B and HepG2 cells independently and additively to those of cisplatin. Ad.RSV-LacZ infection exerted a milder but apparent inhibitory effect on cisplatin-treated hepatoma cells in an Ad dose-dependent manner. Thus, the effects of HGF, Ad and cisplatin on hepatomas were all inhibitory but independent, and, therefore, the Ad.RSV-HGF infection exerted the most prominent inhibitory effects for hepatoma cells as the result of the additive effects of all 3 factors. In contrast, neither Ad.RSV-HGF nor Ad.RSV-LacZ infection changed the effect of cisplatin in HeLa cells.

Discussion

The present study demonstrated not only that adenoviral HGF gene transduction significantly exhibited inhibitory effects on both HCC and hepatoblastoma, but also that such inhibitory effects were due to both the inhibition of cell growth and the induction of apoptosis.

The opposing activities of HGF, i.e., its antimitotic and mitotic effects and its apoptotic and antiapoptotic effects on hepatoma cells and hepatocytes are of biological interest. In terms of effects on cell growth, the following explanations were suggested by recent studies using HepG2 cells. The sustained duration of p21/waf1 induction might be a determinant of HGF-induced inhibitory effects (44), and integrin-mediated signals from the extracellular matrix could modulate HGF-mediated signals (45). The levels of ERK activity might determine the opposing proliferation responses; HGF-induced growth inhibition was caused by the cell cycle arrest, which resulted from hypophosphorylated pRB via high-intensity ERK signals (29). Although HepG2 cells were solely used for these investigations, some of the findings might be applicable to the different phenotypic effects of HGF between hepatoma cells and hepatocytes; hypothetically, the different responsiveness of these molecules might at least in part determine the differences in HGF-induced signaling between them.

In terms of apoptosis and HGF, a recent study interestingly showed the direct interaction of c-Met and the death receptor Fas in hepatocytes; such interaction prevented Fas self-aggregation and Fas ligand binding, thus inhibiting Fas activation and apoptosis (46). Together with the frequent observation of altered Fas expressions and systems in hepatoma cells (47,48), hypothetically, an altered Fas system in